Genomics and reproductive biology of *Leptopilina malgretoutensis* Buffington, Lue, Davis & Tracey sp. nov. (Hymenoptera: Figitidae): An asexual parasitoid of Caribbean *Drosophila*

Amelia RI Lindsey*[1], Chia-Hua Lue[2], Jeremy S. Davis[3], Lydia J. Borjon[4,5], Stephanie E. Mauthner[5], Laura C Fricke[1], Lauren Eads[4], Molly Murphy[4], Melissa K Drown[6,7], Christopher Faulk[6], Matthew L Buffington*[8], W Daniel Tracey Jr*[4,5]

[1]Department of Entomology, University of Minnesota, Saint Paul, Minnesota, USA

[2]Department of Biology, Hood College, Frederick, Maryland, USA

[3]Department of Molecular Biosciences, Northwestern University, Evanston, Illinois, USA

[4]Gill Institute for Neuroscience, Indiana University, Bloomington, Indiana, USA

[5]Department of Biology, Indiana University, Bloomington, Indiana, USA

[6]Department of Animal Science, University of Minnesota, Saint Paul, Minnesota, USA

[7]Current Affiliation: Oxford Nanopore Technologies, New York, New York, USA

[8]Systematic Entomology Laboratory, ARS/USDA c/o Smithsonian Institution, National Museum of Natural History, Washington, DC, USA

*To whom correspondence should be addressed (ARIL: alindsey@umn.edu; MLB: matt.buffington@usda.gov; WDT: dtracey@iu.edu)

ORCIDs:
ARIL 0000-0003-3354-7419
CHL 0000-0002-5245-603X
JSD 0000-0002-5214-161X
LJB 0000-0002-3680-4145
SEM 0000-0002-4159-6571
CF 0000-0002-9749-9658
MLB 0000-0003-1900-3861
WDT 0000-0003-4666-8199

ABSTRACT

Drosophila and parasitic wasps in the genus *Leptopilina* have long been a model for understanding host-parasite interactions. Indeed, parasitic wasps are important drivers of ecological and evolutionary processes broadly, but we are generally lacking information about the diversity, natural history, and evolution of these relationships. We collected insects from the Caribbean Island of Saint Lucia, home to the eastern Caribbean '*dunni*' subgroup of *Drosophila*: a clade long appreciated for its recent patterns of speciation and adaptation. Here we present an integrative approach that incorporates natural history, taxonomy, physiology, and genomics to describe *Leptopilina malgretoutensis* Buffington, Lue, Davis & Tracey sp. nov. (Hymenoptera: Figitidae), a virulent parasitoid of *dunni* group flies, especially *Drosophila antillea. Leptopilina malgretoutensis* is nested within an early-branching clade of *Leptopilina*, offering insights into the evolution of this important genus of *Drosophila* parasitoids. We present a high-quality assembly for this wasp's 1Gbp genome, and for its bacterial endosymbiont: *Wolbachia* strain "*w*Lmal". Furthermore, we show that *w*Lmal induces parthenogenesis in the wasp, and that these wasps are reliant upon their *Wolbachia* infections to produce female offspring. Finally, comparison to historical museum specimens indicate that *Leptopilina malgretoutensis* had been collected approximately 40 years prior from the nearby island of Guadeloupe and were also asexually reproducing. This work represents one of only a handful of studies in which field biology, taxonomy, systematics, genomics, and experimental biology are integrated into a species description: showcasing the possibilities for biodiversity research in the genomic era.

KEYWORDS

dunni, *cardini*, *Wolbachia*, parthenogenesis, Saint Lucia, Antilles, host-parasite

INTRODUCTION

Interactions between insects and their parasitoids are ubiquitous across terrestrial ecosystems, and have been postulated as critical, but underappreciated, drivers of ecological speciation in insect groups [1, 2]. Yet compared to other ecological interactions, considerably less attention is paid to parasitism as a driver of insect speciation, in part because of the challenges of identifying often cryptic parasitoid species. Molecular-based identification methods have rapidly revolutionized species identification, but issues persist for many parasitoid lineages [3]. Most critically, while parasitoids are commonly acknowledged as one of the most speciose groups of organisms, they are persistently under-described and under-represented in insect conservation efforts [4-6]. As such, more effort to find and describe the ecology and unique biology of new parasitoid species is needed to better understand the pattern and scope of biodiversity on earth.

Island species groups have been attractive systems for the study of speciation events and adaptive radiations since as far back as Darwin (1859), who recognized the immense number of endemic species on archipelago chains. Island archipelagos offer unique opportunities to study peripatric speciation following discrete patterns of colonization between single islands in an archipelago chain [7]. *Drosophila* species groups have been of particular interest for studying patterns of island colonization and speciation. Indeed, the Hawaiian *Drosophila* group represents one of the most well studied examples of island radiations – home to at least 500 species and research spanning decades [8-10]. While Hawaiian *Drosophila* are the most intensely studied group, several other island clades of *Drosophila* have received research attention (e.g., *sechellia-simulans* [11, 12]). Another such clade is the *D. dunni* group – a subgroup of the larger *D. cardini* group that is endemic to the Caribbean islands, particularly the Lesser Antilles [13, 14]. This subgroup is characterized by species or subspecies with distinct abdominal pigmentation endemic to just one or two major islands in this archipelago – frequently just 25-50 km apart. As such, this group represents an excellent model for the study of peripatric speciation and morphological evolution across archipelagos [12, 14]. Despite years of appreciation for the *dunni* group as a model, little is known about the parasitoid complex of these Caribbean flies.

To better understand the ecology of *dunni* group *Drosophila,* and to investigate their potential parasitoids, we (JSD, SEM, WDT) conducted an expedition to the islands of the Lesser Antilles February through May of 2019. We traveled among the islands aboard the sailing vessel Sea Salt (a 42-foot Fountaine Pajot Catamaran) which also served as a mobile laboratory. We describe here results with collected flies and associated parasitoids from the island of Saint Lucia. Other results of our expedition will be described elsewhere. We describe a new species of *Drosophila* parasitoid: *Leptopilina malgretoutensis* Buffington, Lue, Davis & Tracey sp. nov. (Hymenoptera: Figitidae). *Leptopilina malgretoutensis* appears to be endemic to the Lesser Antilles and we find that it has high virulence against *dunni* group flies, particularly *Drosophila antillea* also collected on Saint Lucia. To our knowledge, this is the first host-parasitoid association recorded for *cardini* and *dunni* group *Drosophila.* We find that the wasps reproduce via thelytokous parthenogenesis (the asexual reproduction of females) and that this is caused by infection with a bacterium: a parthenogenesis-inducing *Wolbachia* symbiont. We report *de novo* genome assemblies for *Leptopilina malgretoutensis* and its *Wolbachia* strain, hereinafter "*w*Lmal". *Leptopilina malgretoutensis* has the largest *Leptopilina* genome reported to-date (~1Gbp) and will serve as a useful resource for understanding the evolution of *Drosophila*-*Leptopilina* relationships in the Caribbean islands, island speciation events, and parasitoid genome evolution more broadly.

METHODS

Collection: Field sites and field rearing

After sailing from Wallliabou Bay of Saint Vincent and the Grenadines, we moored the research vessel and operated out of Soufrière and Marigot Bays of Saint Lucia. Verbal permission for collection of *Drosophila* and their parasitoids was obtained in a February 2019 meeting with Dr. Hannah Romain of the Saint Lucia Ministry of Agriculture. Sampling was conducted in 2019 on Saint Lucia and leveraged baited trapping with either banana or calabasa, a locally available cucurbit fruit (likely *Cucurbita moschata*). Calabasa and banana traps contained chopped fruit mixed with water and baker's yeast that had been kept in a closed bucket for one or more days to ferment. The Calabasa bait was chosen based on communication with Hope Hollecher who found it to be particularly attractive to *dunni* group *Drosophila.* Traps were set at two separate sites from which flies and wasps in this study derive. The first site, known

as STL3 was placed on 24 February 2019 with a total of 2 calabasa traps on a short trail leading off the main road near Ladera resort and Hotel Chocolat (GPS: lat 13.83, lon -61.05, elevation 289.6m, Figure 1). The second site, known as STL6 was placed on 26 February 2019 with a total of eight traps (5 calabasa, 3 banana) along Barre d'Isle trail (GPS: lat 13.924, lon -60.959, elevation 308.7m, Figure 1). Each trapping site was checked daily for three days and insects were collected off the fruit each time. Flies were collected using either cardboard mailing tubes for vertical trapping or mouth aspiration, and wasps were collected by mouth aspiration while they searched for larvae in the bait.

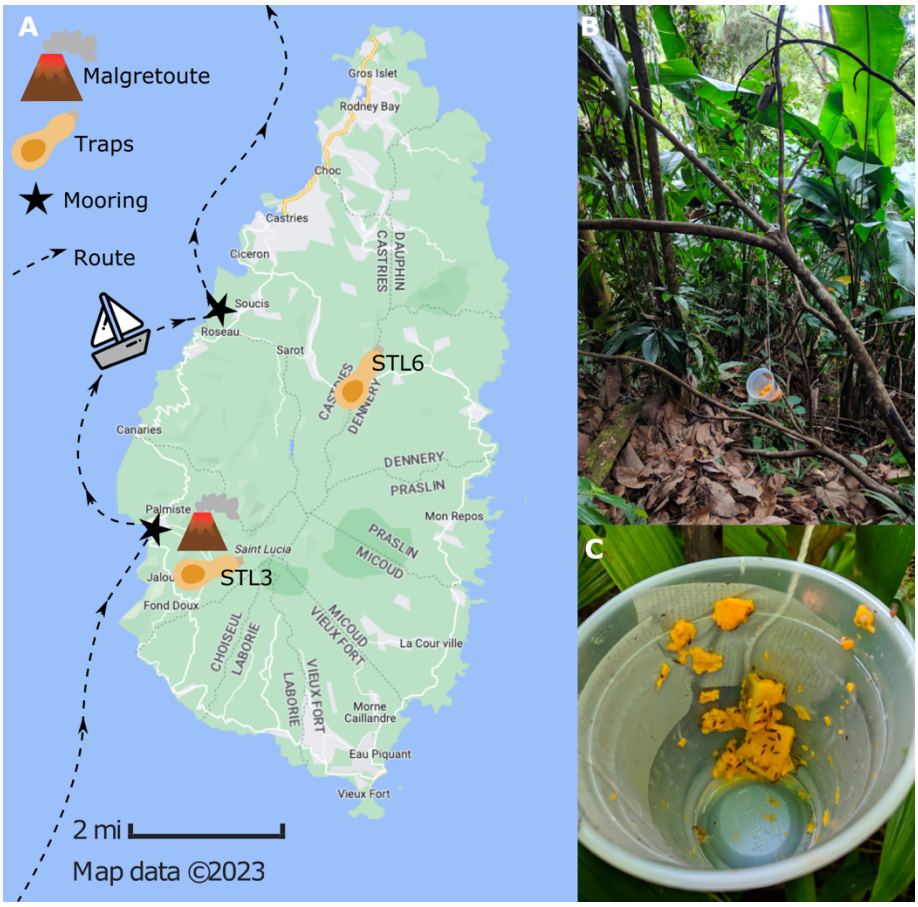

Figure 1. Collections on Saint Lucia: field notebook entry from JSD on 1 March 2019: "*...a 40-minute brisk hike, in which I found 0 wasps in the traps - [bummer]. Until I remembered I had set out one more trap off the path a little that I had not checked yet. And [nevertheless], my lucky [telson] finds the wasp we needed sitting in this cup. I managed to nab it and was pretty excited leaving here.*" **(A)** Map of Saint Lucia (GoogleMaps 2023), annotated with (1) locations of the STL3 and STL6 trap placements, (2) the route and mooring locations (Soufrière in the south, and Marigot in the north) of the Sea Salt, and (3) Malgretoute: the location of the La Soufrière Volcano. **(B)** The STL6 calabasa trap. **(C)** The inside of a calabasa trap.

127 **Collection: Colony establishment and maintenance**

128 After collection, flies and wasps were transferred to individual rearing vials with instant fly media (Formula
129 4-24® Instant Drosophila Medium, Blue; Carolina Biological Supply Company). Isofemale lines of
130 *Drosophila antillea* and *Drosophila willistoni*, were initiated using flies collected at STL3 (see results). A
131 single wasp was collected from STL6 and was left in a vial with developing STL3 *Drosophila willistoni*
132 larvae. This vial was then shipped back to Indiana University Bloomington under USDA APHIS
133 Importation Permit Number P526P-19-01355. Since 2019, wasps have been maintained continuously on
134 host cultures of *D. willistoni* on Bloomington fly food medium and further reared in IU USDA regulated
135 containment facility number 5035.

136

137 **Taxonomy: Imaging**

138 Voucher specimens were sent to two of us (CHL and MB) for identification. These specimens were
139 compared with specimens deposited in the USNM as well as those on loan from Goran Nordlander
140 (Uppsala Agricultural University, retired). Additionally, notes from Yves Carton were shared with MB, and
141 his work with G. Nordlander in the mid 1980's. These notes revealed an undescribed *Leptopilina* from
142 Guadeloupe that matched the species described herein. We are therefore including these older
143 specimens in the description. Images were acquired using a Hitachi 3000 desktop Scanning Electron
144 Microscope (SEM), after a 120nm coating of Au-Pd from a Cressington sputter-coater. Light micrographs
145 were shot using a Macropod 3D Pro camera setup. All type specimens collected in this study are housed
146 in the USNM (registration numbers below); additional types, examined by G. Nordlander, reside in the
147 Uppsala Agricultural University collection overseen by G. Nordander. Terminology for these descriptions
148 follows Lue et al. (2016) [15].

149

150 **Taxonomy: Systematics of *Leptopilina***

151 Lue et al. (2016) [15] provided a detailed description on the species limits of *Leptopilina*. Species in this
152 genus are common throughout the Holarctic Region and have recently been investigated for their
153 biological control potential of pestiferous Drosophilidae [16, 17]. Some 29 species are currently
154 recognized worldwide [15]. While most described species are endemic to the Holarctic Region, many

155 undescribed species remain in collections, awaiting description. A relatively common trait among
156 Neotropical *Leptopilina* are polychromatic antennal segments, specifically black/brown, cream, and
157 orange-colored segments. These traits are either rare, or wholly missing, from the Paleotropics and
158 Australia (Buffington, Lue, pers. obsv.). This is mentioned here as the new species, herein described, has
159 rather unique color patterns among the antennal segments. This character makes this species relatively
160 straightforward to diagnose from other *Leptopilina*.
161
162 **Biology: Virulence assessment**
163 To test the virulence of *L. malgretoutensis* on *Drosophila* host species, infection vials were established at
164 a wasp-to-larvae ratio of 1:10 (typically 5 female wasps and 50 drosophila larvae). Two isofemale lines
165 from two *Drosophila* species that were collected from the island of Saint Lucia were assessed: *Drosophila*
166 *willistoni* (line STL3 iso3) and *Drosophila antillea* (line STL3 iso1). To collect the age-matched larvae, 20-
167 30 male and female adult flies were placed in embryo collection cages. The embryo collection plates (60
168 x 15mm) contained 5mL of *Drosophila* banana food medium (Archon Scientific) and a small amount of
169 yeast paste (active dry yeast mixed with water). The embryo collection cages were maintained in an
170 incubator set at 25°C and 75% humidity on a 12h/12h light/dark cycle. Embryos from a restricted 12-hour
171 egg-laying window were allowed to develop in the incubator for 3 days until they reached the size of 2nd
172 instar larvae. Larvae were carefully gently collected using extreme caution so as to not damage them.
173 Fifty larvae were placed into individual vials containing *Drosophila* banana food and a small cotton dental
174 plug that was inserted into the center of the food. The cotton plug was necessary to provide a place for
175 pupariation for the *D. antillea* species (which avoids pupariation on the side of the culture vials). Five
176 naïve *L. malgretoutensis* female wasps were placed into each infection vial and were allowed to infect the
177 larvae for 24 hours. During the infection period, the vials were closed with Flugs (Genesee Scientific
178 cat.no.49-102) dampened with honey and water (1:1 mixture) to ensure that the wasps had access to
179 food. After the infection period, the wasps were removed, and the vials were incubated as described
180 above. Uninfected mock control vials were treated in the same way but were not exposed to wasps. The
181 vials were assessed daily for the emergence of adult insects. Adult flies eclosed after 10-14 days, and
182 adult wasps eclosed after 25-30 days. Any newly eclosed adult flies and wasps were counted and

183 removed from the vials. The difference between the total number of adults and the initial number of larvae
184 in each vial accounts for larval mortality.
185
186 **Biology: Western blots for *Wolbachia* detection**
187 Active *Wolbachia* infection was assessed with western blot following published protocols [18]. Positive
188 and negative controls included individual *Drosophila melanogaster* from previously validated *Wolbachia*-
189 infected and -uninfected stocks (RRID: BDSC_145) [19]. Individual insects were homogenized with a
190 pestle in 1.7 ml microcentrifuge tubes containing lysis buffer (150mM NaCl, 1% Triton X-100, 50mM
191 TrisHCl (pH8) containing HALT protease inhibitor cocktail (Thermo Scientific) and 5 mM EDTA).
192 Homogenates were pelleted via centrifugation (8,000Xg for 1 minute) and the supernatant was incubated
193 for 5 minutes at 95°C in Laemmli sample buffer with 5% β-mercaptoethanol (Bio-Rad). Proteins were
194 separated via SDS-PAGE on 4–20% Tris-Glycine gels (NuSep) in 1X Tris/Glycine/SDS running buffer
195 (Bio-Rad) alongside a PageRuler prestained protein ladder (Thermo Scientific), transferred to a PVDF
196 membrane in Tris-Glycine transfer buffer with 15% methanol for 3 hours at 40v, and blocked for 5 minutes
197 in Starting Block T20 (Thermo Scientific). The membrane was co-incubated in primary antibodies
198 overnight at 4°C. After washing, the blot was incubated with the secondary antibody anti-mouse:HRP
199 (Invitrogen) at 1:5000. Finally, HRP was detected with SuperSignal West Pico Chemiluminescent
200 Substrate (Thermo Scientific). Primary antibodies included (1) mouse monoclonal Anti-Wolbachia Surface
201 Protein (WSP), NR-31029 from BEI Resources, NIAID, NIH at 1:10,000, and (2) mouse anti-actin
202 monoclonal at 1:20,000 (Seven Hills Bioreagents) as a loading control.
203
204 **Biology: Determining reproductive mode**
205 To test whether the observed parthenogenesis was induced by infection with a bacterial symbiont, *L.*
206 *malgretoutensis* female wasps were fed with the antibiotic rifampicin mixed into honey (100 mg of
207 rifampicin powder (Sigma-Aldrich cat.no. R3501-250MG) with 1 mL of honey) and reproductive biology
208 was assessed following standard protocols [20]. To feed the wasps, a Flug was dipped into water to
209 dampen one side, onto which a small amount of the rifampicin-honey mixture was spread (approx. 10-20
210 μL). A fresh Flug with rifampicin-honey was replaced once a day for six days. To prepare vials of fly

211 larvae, adult *Drosophila* were allowed to seed vials for 5 days, after which the adults were removed. After
212 the six days of rifampicin treatment, the treated wasps were placed into the vials with fly larvae and
213 allowed to infect as many larvae as possible. Wasp offspring eclosed after 25-30 days and all female and
214 male offspring were collected and counted. Rifampicin treatment trials were performed with larval hosts
215 from fly species that were collected on the island of Saint Lucia, either *D. melanogaster* or *D. willistoni*.
216 Regardless of the host species, the sex ratio of the wasp offspring in each generation was always almost
217 all female or almost all male (see results, Figure 5), and therefore the data from the trials with different
218 host species were combined. The treatment conditions of each generation were as follows: G_1 unmated
219 females received 6 days of rifampicin treatment. The G_2 offspring were almost all female and also
220 received 6 days of rifampicin treatment, after which they produced F_0 offspring. In order to cross
221 *Wolbachia* depleted males and females together, a separate generation of G_1 females was treated with
222 rifampicin to produce G_2 females that would eclose at the same time as the F_0 males. These G_2 females
223 then received 6 days of rifampicin treatment and were then mated to F_0 males. Subsequent generations
224 (F_1 - F_5) were sexed and propagated by attempting sibling mating (when possible, see results) without
225 further rifampicin treatments.
226
227 **Genomics: Oxford Nanopore library preparation and sequencing**
228 DNA was extracted from a pool of ~100 adult female wasps using a Gentra PureGene Tissue Kit
229 (Qiagen). 3 ug of DNA was end prepped using NEBNext FFPE Repair Mix (M6630), NEBNext Ultra II End
230 repair/dA-tailing Module (E7546), and NEBNext Quick Ligation Module (E6056) and subsequently library
231 prepped using the ONT supplied SQK- LSK110 kit. Sequencing took place on an Oxford Nanopore
232 Minion over 3 days with nuclease wash followed by reloading after 24 hours. The sequencing computer
233 was built with an AMD Ryzen 3900x processor with 12 threads, 24 cores, 64 Gb RAM and a 1 Tb SSD,
234 and a GeForce 2080Ti with 4352 CUDA cores running Ubuntu Linux 20.04. We monitored the CUDA
235 cores with nvtop (https://github.com/Syllo/nvtop). Fastq files were generated from the Oxford Nanopore
236 Minion instrument and called with Guppy v6.1.5. We used the GPU enabled version of guppy in concert
237 to enable live basecalling with the fast base calling model and for post-hoc base calling with the super

238 (sup) accuracy model called via Minknow v22.05.5. All resulting fastq.gz files were concatenated and
239 used for further processing.
240
241 **Genomics: Illumina sequencing**
242 Total DNA was extracted from a pool of ten adult wasps using the DNeasy blood and tissue kit (Qiagen).
243 Sequencing library preparation was performed with the NEBNext Ultra II DNA library preparation kit (New
244 England Biolabs) according to the manufacturer's protocols including 10 cycles of PCR amplification. The
245 resulting library was subjected to 150-bp paired-end sequencing on the Illumina NextSeq 500 platform at
246 the Indiana University Center for Genomics and Bioinformatics (Bloomington, IN) to generate
247 181,561,108 read pairs. To aid in gene annotation we also sequenced wasp transcriptomes. Total RNA
248 was extracted from a flash-frozen, mixed stage pool of 10 wasps (adults, pupae, larvae) using the
249 Monarch® Total RNA Miniprep Kit (New England Biolabs) including the DNase treatment step. An RNA-
250 Seq library was prepared with the Illumina TruSeq Stranded mRNA Library Prep Kit, including rRNA
251 removal with oligo-dT beads, and sequenced on a NovaSeq with S4 chemistry at the University of
252 Minnesota Genomics Center to generate 64,677,726 150-bp paired-end reads.
253
254 **Genomics: Nuclear genome assembly, curation, and quality control**
255 All reads greater than 5kb were filtered with SeqKit v2.5.1 [21], assembled with Flye v2.9 [22], and the
256 assembly was polished with Medaka v1.5.0 (https://github.com/nanoporetech/medaka). Haplotigs were
257 purged with PurgeHaplotigs v1.1.2 [23]. Pilon v.1.22 [23] was used for polishing: first WGS Illumina reads
258 were mapped to the long-read assembly with bwa v0.7.17 [24], alignment files were converted and sorted
259 with samtools v1.10 [25], and finally pilon was called for polishing to generate an updated assembly. Four
260 rounds of pilon polishing were performed, each time mapping the short reads to the most recent pilon
261 output prior to pilon correction. Manual curation of the assembly and identification of cytoplasmic
262 genomes was informed by results derived from running blobtools [26]. We discarded contigs that were
263 deemed anomalous for the following reasons: (1) less than 5,000 bp in length with no BUSCOs (because
264 >5k reads were used during assembly, these are very likely to be chimeric and/or haplotigs), or, (2)
265 having blast hits to non-arthropod taxa across the length of the contig, unusual sequencing

266 coverage(<15X; >800X), and unusual GC content (outside of 23-33%). Next, we checked the previously
267 purged contigs and recovered those that appeared to encode for *Leptopilina* rRNAs. Assemblies were
268 assessed with BUSCO v.5.3.2 [27] against the hymenoptera_odb10 database in genome mode ('-m
269 genome'). Finally, NCBI's Foreign Contamination Screen (FCS) was used to detect and remove other
270 contaminants [28]. Specifically, a small number of adaptor sequences were found and trimmed from the
271 ends of contigs. Three contigs had adaptor sequence in the middle (>5,000 bp from the ends): for these,
272 the adaptor sequence was removed and the contig split into two separate contigs, as per NCBI/FCS
273 recommendations [28].
274
275 **Genomics: Methylation**
276 Nanopore runs were base called with guppy v6.3.8 using model
277 "dna_r9.4.1_450bps_modbases_5mc_cg_sup" to call 5-methylcytosines in a CpG context only. Aligned
278 bam reads containing modified base information were converted into bed format with modbam2bed, with
279 strict parameters on canonical and modified base probabilities where bases are only called as canonical
280 or modified if they have a greater than 95% probability estimate. Parameters: modbam2bed -m 5mC -t 32
281 -e -p total.modmapped --aggregate --cpg dtwasp-final-curated.fa total.modmapped.bam -a 0.05 -b 0.95 >
282 total.modmapped.bed". Global methylation was calculated by an awk script.
283
284 **Genomics: Mitogenome**
285 Mitogenome annotation with MITOS2 [29] and manual rearrangement to start the circular mitogenome at
286 Cox1 (as is convention) was done as in [30]. MITOS2 parameters included the RefSeq 63 Metazoa
287 reference and the invertebrate mitochondrial translation code. Manual curation was facilitated by
288 comparison to published mitochondrial genomes from *Leptopilina boulardi* (KU665622.1) and *Leptopilina*
289 *syphax* (MT649407.1). A phylogeny of *Leptopilina* was constructed based on COX1 ("COI") sequences
290 available from the DROP database [3]. A subset of the available *Leptopilina* sequences were selected
291 based on (1) sampling across the genus, (2) limiting the total number of sequences for any given species,
292 (3) length of the barcoding region sequenced, and (4) checking for open reading frame. In total 55
293 sequences were used for phylogenetic reconstruction. These include an outgroup (*Ganaspis kimorum*),

294 previously sequenced barcodes for the *Leptopilina malgretoutensis* STL6 colony [3], and the COI
295 sequence derived from the mitogenome assembly. Nucleotide sequences were aligned with MAFFT
296 v7.511 [31] using the L-INS-i alignment algorithm and a five point gap open penalty (-op 5). Comparison
297 to the translated amino acid alignment verified that codon relationships were maintained and we did not
298 need to back-translate an amino acid alignment. Ends of the nucleotide alignment were trimmed such that
299 all sequences were represented at all positions. Phylogenetic reconstruction was then performed with
300 IQtree v1.6.11 [32] using a pre-analysis model optimization step to select the final model (here,
301 TIM3+F+I+G4) plus 1000 "ultrafast" bootstraps.
302
303 **Genomics: Repeat identification**
304 Repetitive DNA content was estimated using RepeatModeler2 [33] using the curated Dfam database
305 release 3.5 July 2021 [34], combined with the Repbase RepeatMasker database downloaded on October
306 26, 2018. RepeatMasker was run with the newly identified library to annotate the assembly with the
307 following parameters: RepeatMasker v4.1.2-pl -pa 24 -s [sensitive mode] [using rmblast 2.11.0+] -lib
308 ultimatefamilies.fa ultimateGenome.fasta. Each repeat library was also mapped against all other species
309 genomes with the following parameters: RepeatMasker v4.1.2-pl -pa 24 -s [sensitive mode] [using rmblast
310 2.11.0+] -lib families.fa genome.fasta.
311
312 **Genomics: Gene annotation and ortholog clustering**
313 Gene models were predicted with GeMoMa v1.9 [35] and leveraged three lines of evidence: (1) RefSeq
314 annotations for *Leptopilina heterotoma* (GCF_015476425.1) (2) RefSeq annotations for *Leptopilina*
315 *boulardi* (GCF_019393585.1) and (3) RNA-seq reads derived from the mixed pool of wasps. RNA-seq
316 reads were mapped to a hard masked version of the reference genome using STAR v2.5.3a [36].
317 GeMoMa was called with the following additional parameters: tblastn=TRUE, AnnotationFinalizer.n=false,
318 AnnotationFinalizer.r=SIMPLE, AnnotationFinalizer.t=true, AnnotationFinalizer.p=LMAL, pc=true, o=true.
319 To generate annotations for *Leptopilina clavipes* and *Ganaspis kimorum*, we ran the same annotation
320 pipeline on hard-masked assemblies, only without the RNA-seq data. Protein sequences from each

321 genome were clustered into orthologous groups using OrthoFinder v.2.5.4 [37]. For genes represented by
322 multiple transcript variants, only the longest isoform was used in clustering.
323
324 **Genomics: *Wolbachia* genome**
325 A single contig was identified to be a *Wolbachia* genome, based on size, circularity, and Blobtools results.
326 Genome completeness was assessed with BUSCO v5.3.2 [27] against the rickettsiales_odb10 database
327 in genome mode ('-m genome'). Genome annotation and phylogenetics were performed by running the
328 *Wolbachia* Phylogeny Pipeline (WHOP; https://github.com/gerthmicha/WHOP [38]). In brief, the pipeline
329 takes a provided database of bacterial genomes (*Wolbachia* strains and Rickettsiales outgroups) plus
330 additional genomes provided by the user, annotates them with Prokka v1.14.6 [39], clusters protein
331 sequences into orthogroups with OrthoFinder v2.5.4 [37], aligns the single-copy orthologs with MAFFT L-
332 INS-i v7.487 [31], removes recombining genes with PhiPack v1.1 [40], and then concatenates the
333 alignments prior to phylogenetic reconstruction with IQtree v2.2.3 [32]. IQtree was first run with a pre-
334 analysis model optimization step (-m LG+I+G4 -pre -redo -fast), followed by final reconstruction with the
335 selected model and 1000 bootstrap replicates. The *w*Lmal genome was re-oriented to start at *dnaA* and
336 proksee (https://proksee.ca/ [41]) was used for visualization. Prophage regions were identified with
337 VirSorter2 v.2.2.4 [42], and Phigaro v.2.3.0 [43], and other mobile elements were identified with
338 mobileOG-db v.1.0.1 [44], all implemented in proksee with default parameters. To aid in manual
339 annotation of *w*Lmal we leveraged the orthogroup relationships between *w*Lmal and *w*Mel generated by
340 WHOP to check for specific proteins. Additionally, we used blastp and tblastn with default parameters to
341 query against the protein sequences or genome, respectively, for a select number of functionally relevant
342 *Wolbachia* proteins not found in *w*Mel. All manual annotation queries and matches are in Supplemental
343 Tables S5-6.
344
345 **Data visualization**
346 Data visualization was carried out in R version 4.1.3 [45] and leveraged Paul Tol's "Medium-contrast
347 qualitative colour scheme", (R: khroma [46]). Newick files from phylogenetic reconstructions were
348 visualized in FigTree v1.4.4 (https://github.com/rambaut/figtree/) and annotated in Inkscape. Proksee

349 (https://proksee.ca/ [41]) was used for genome visualization, and the r package 'gggenes' v.0.5.1 was
350 used to plot gene models.
351
352 **RESULTS**
353 **Collections on Saint Lucia**
354 Banana and calabasa fruit traps were used to collect *Drosophila* and their associates on Saint Lucia in
355 2019. The calabasa traps at STL3 yielded six female *Drosophila antillea* and one female *Drosophila*
356 *willistoni.* Isofemale lines of *D. antillea* and *D. willistoni* were established from single females that
357 originated from the STL3 collection site. At site STL6, banana traps contained a total of 12 *melanogaster*-
358 like flies and 1 *repleta* group fly. Calabasa traps contained 4 *melanogaster*-like flies, 4 *repleta* group flies
359 and 20 *dunni*-group flies. Wasp "STL6" was collected from a calabasa trap on the morning of 1 March
360 2019: a clear day with a high temperature of 27C (Figure 1). The STL6 wasp was placed in a vial with
361 developing *Drosophila willistoni* (from the STL3 site, see above) to initiate a culture, and then shipped
362 back to Indiana University where they have been maintained since (see methods).
363
364 ***Leptopilina malgretoutensis* Buffington, Lue, Davis & Tracey sp. nov.**
365 **Species Diagnosis**. *Leptopilina malgretoutensis* is distinguishable from other *Leptopilina* species by a
366 number of characters, including: flagellomere colors, in which F1-F4 are honey-brown, F5-F10 are dark
367 brown, and F11 is yellow (Figure 2A); the typical flagellomere color in *Leptopilina* do not match the unique
368 combination here. Latero-posterior margin of pronotal plate is with elongate, golden setae that reach the
369 anterior margin of the mesoscutum (Figure 2B (LM) and Figure 3A-B (SEM)). No other known *Leptopilina*
370 have setae so long off the pronotal plate (Figure 2B); other species have hairs here, but not so long.
371 Members of the *clavipes* group *sensu* [15] tend to also have sparse, scattered setae over the
372 mesoscutum, whereas *L. malgretoutensis* is entirely glabrous (Figure 3A-B).
373
374 **Morphological Description**
375 Coloration with head, mesosoma, metasoma black to dark brown, legs light brown. Sculpture on vertex,
376 lateral surface of pronotum and mesoscutum absent, surface smooth.

Antenna. Female antenna composed of scape, pecidel, 11 flagellomeres (F1-F11). F1-F4 sub-cylinderical, slightly expanded distally, smooth, non-claval segments. F5-F11 claval segments, abruptly broader than non-claval segments, distinctly barrel-shaped, with slightly more erect, dense setae; claval segments with placoidal sensillae distributed evenly around each segment. Single campaniform sensillae present ventro-apically on F6-F10 (arrow, Figure 3C; compare to Figure 3D). Articulation between flagellomeres in antenna moniliform, segments distinctly separated by narrow neck-like articulation. Male antenna composed of 13 flagellomeres, F1 as long as F2, slightly curved and excavated distally; campaniform sensillae on all flagellomeres.

Head. In anterior view, broadly triangular. Pubescence on head sparse, single setae scattered over face. Sculpture along lateral margin of occiput absent. Gena (measured from compound eye to posterolateral margin of head) short, ratio of length of gena to length of compound eye in dorsal view <0.3. Sculpture of gena absent, smooth. Lateral margin of occiput evenly rounded, not well defined. Occiput (except extreme lateral margin) smooth. Carina issuing from lateral margin of postocciput absent. Ocelli small, ratio of maximum diameter of a lateral ocellus to shortest distance between lateral ocelli 0.2-0.4. Anterior ocellus far from posterior ocelli, clearly separate anterior ocellus to anterior margins of posterior ocelli. Relative position of antennal sockets intermediate, ratio of vertical distance between inner margin of antennal foramen and ventral margin of clypeus to vertical distance between anterior ocellus and antennal rim 2.0-4.0. Median keel absent. Vertical carina adjacent to ventral margin of antennal socket absent; facial sculpture absent, surface smooth. Facial impression absent, face flat. Antennal scrobe absent. Anterior tentorial pits small. Vertical delineations on lower face absent. Ventral clypeal margin laterally, close to anterior mandibular articulation, straight. Ventral clypeal margin medially straight, flat, with 4-6 setae overhanging base of mandibles. Clypeus smooth. Malar space adjacent to anterior articulation of mandible evenly rounded, smooth. Malar sulcus present, composed of single groove. Eye removed from lateral ocelli, ratio of distance between compound eye and posterior mandibular articulation to distance between posterior ocellus and compound eye <1.2. Compound eyes, in dorsal view, moderately protruding from the surface of the head. Pubescence on compound eyes absent. Orbital

furrows absent. Lateral frontal carina of face absent. Dorsal, posterior aspect of vertex smooth. Hair punctures on lateral aspect of vertex absent. Posterior surface of head deeply impressed around postocciput.

Mouthparts. Apical segment of maxillary palp with pubescence, consisting of one long erect setae. Apical seta on apical segment of maxillary palp longer than twice length of second longest apical seta. Maxillary palp composed of four segments. Last two segments of maxillary palp (in normal repose) straight. Apical segment of maxillary palp about 1.5 times as long as preceding segment. Left mandible with three teeth; scattered setae dorsally.

Mesosoma. Long auburn-golden setae present, originating from anterior inflection of pronotum, extending to anterior margin of mesoscutum; rest of pronotum glabrous (Figure 3A-B). Anteroventral inflection of pronotum narrow. Pubescence on lateral surface of pronotum absent. No ridges present posterior to pronotal plate. Anterior flange of pronotal plate distinctly protruding anteriorly, completely smooth. Ridges extending posteriorly from lateral margin of pronotal plate absent. Lateral pronotal carina absent. Crest of pronotal plate absent. Dorsal margin of pronotal plate (in anterior view) spatulate. Submedian pronotal depressions open laterally, deep. Lateral margin of pronotal plate defined all the way to the dorsal margin of the pronotum. Width of pronotal plate narrow, not nearly as wide as head.

Mesoscutal surface convex, evenly curved. Sculpture on mesoscutum absent, entire surface smooth, shiny, with sparse long hairs. Notauli absent. Median mesoscutal carina absent. Anterior admedial lines absent. Median mesoscutal impression absent. Parascutal carina nearly straight.

Mesopleuron entirely smooth. Subpleuron entirely smooth, glabrous. Lower pleuron entirely smooth, glabrous. Epicnemial carina absent. Lateroventral mesopleural carina present, marking abrupt change of slope of mesopectus. Mesopleural triangle absent. Subalar pit not visible. Speculum absent. Mesopleural carina present, complete, composed of one complete, uninterrupted carina. Anterior end of mesopleural

carina inserting above notch in anterior margin of mesopleuron; posterior end terminates at setal pit of lower metapleuron.

Dorsal surface of scutellum foveate-areolet (Figure 3E). Circumscutellar carina present, complete, delimiting dorsal and ventral halves of scutellum. Posterior margin of axillula marked by distinct ledge, axillula distinctly impressed adjacent to ledge. Latero-ventral margin of scutellum, posterior to axillula, weakly rugulose. Dorsoposterior part of scutellum rounded. Transverse median carina on scutellar plate absent. Dorsal part of scutellum entirely areolate. Scutellar plate, in dorsal view, medium sized, exposing about half of scutellum, gently foveate with three to four single setae; glandular release pit at posterior end, oval. Scutellar fovea present, two, distinctly margined posteriorly, smooth. Longitudinal scutellar carinae absent. Single longitudinal carina separating scutellar foveae present, elongage, ending past posterior margin of foveae, gently expanding into teardrop-shaped scutellar plate. Postero-lateral margin of scutellum rounded. Lateral bar smooth, narrow.

Posterior impression of metepimeron absent. Metapectal cavity anterodorsal to metacoxal base present, well-defined (Figure 3F, arrow A). Anterior margin of metapectal-propodeal complex meeting mesopleuron at same level at point corresponding to anterior end of metapleural carina. Posteroventral corner of metapleuron (in lateral view) not extended posteriorly. Anterior impression of metepimeron absent. Posterior margin of metepimeron distinct, separating metepimeron from propodeum, with distinct ridge (Figure 3F, arrow B). Anteroventral setal pit of lower metapleuron present, with foamy setae. Subalar area broadened anteriorly, narrowed posteriorly. Prespiracular process present, blunt, lobe-like, polished, at end of polished prespiracular groove; posteroventral corner of prespiracular groove extended to distinct lobe. Dorsellum absent. Anterior impression of metepisternum, immediately beneath anterior end of metapleural carina, present. Pubescence consisting of few hairs on posterior part of metepisternum, few sparse hairs on propodeum, but with distinct posterior swatch of foamy setae at midline of metapleuron.

Pubescence posterolaterally on metacoxae sparse, with a single postero-dorsal button of dense pubescence. Microsculpture on hind coxa absent. Longitudinal ridge on the posterior surface of metatibia absent. Metafemoral tooth present, elongate, with adjacent serrate ridge posteriorly. Ratio of first metatarsal segment to remaining 4 segments less than 10; metatarsus 5 distinctly elongate relative to 2 through 4.

Wing vein M absent. Pubescence of fore wing present, long, moderately dense on most of surface. Apical margin of female fore wing rounded. Rs+M of forewing defined but nebulous at point of origin from basal vein at posterior third. Mesal end of Rs+M vein situated closer to anterior margin of wing, directed towards middle of basalis. Vein R1 forming marginal cell completely. Basal abscissa of R1 (the abscissa between 2r and the wing margin) of fore wing as broad as adjacent wing veins. Coloration of wing absent, entire wing hyaline. Marginal cell of fore wing membranous, similar to other wing cells. Areolet absent. Hair fringe along apical margin of fore wing present, long or very long (Figure 2C).

Propodeal spurs absent. Lateral propodeal carinae present, not reaching scutellum. Ventral end of lateral propodeal carina reaching nucha, carinae separated from each other, elbowed at midpoint, not parallel. Inter propodeal carinae space lightly setose, underlying surface appearing smooth. Petiolar rim of uniform width along entire circumference. Petiolar foramen removed from metacoxae, directed posteriorly. Horizontal carina running anteriorly from lateral propodeal carina absent, moderately setose. Calyptra, in lateral view, rounded. Propodeum not strongly drawn out posteriorly. Calyptra, in posterior view, dorsoventrally elongate or rounded.

Metasoma. Petiole about as long as wide. Surface of petiole longitudinally costate, ventral keel absent. Posterior part of female petiole abruptly widened. Ventral and lateral parts of petiolar rim broad.

Setal band (hairy ring) at base of tergum 3 present, interrupted dorsally, ventrally. Tergum 3 indistinct, fused with syntergum. Posterior margin of tergum 3 indistinct, fused with tergum 4 in syntergum. Posterior margin of tergum 4 evenly rounded. Sternum 3 encompassed by syntergum. Sculpture on metasomal

terga absent. Syntergum present with terga 3 to 5 fused, ventral margin rounded. Peglike setae on T6-T7 absent. Postero-ventral cavities of female metasoma T7 present, glabrous save for few, long setae. Female postero-ventral margin of T6-T7 straight, parallel. Terebrum and hypopygium (in lateral view) curved, pointing upward. Ovipositor clip present.

Etymology. The species epithet refers to locations on Saint Lucia: Malgretoute, a town near the island's active volcano, and the near-by Malgretoute Beach, from which the iconic Saint Lucia Pitons are visible.

Material examined. Holotype: Female. Saint Lucia, Barr d'Isle trail, central. lat 13.924, long -60.959, elevation 308.7m. 17.II.2019, Jeremy S. Davis, collected from calabasa bait trap. USNMENT01025555. [1] Actual specimen taken from Indiana University colony derived from the above collection locality.

Paratypes: 9 females, 3 males. Same collection data as holotype. USNMENT01557161, USNMENT01025556, USNMENT01025557, USNMENT01025554, USNMENT01557162, USNMENT01557158, USNMENT01448469, USNMENT01448467, USNMENT01932975-USNMENT01932978.

Other material examined. 8 females. INRA laboratory, Petit Bourg, Guadeloupe, January 1982. Carton, coll. USNMENT01025775-USNMENT01025782

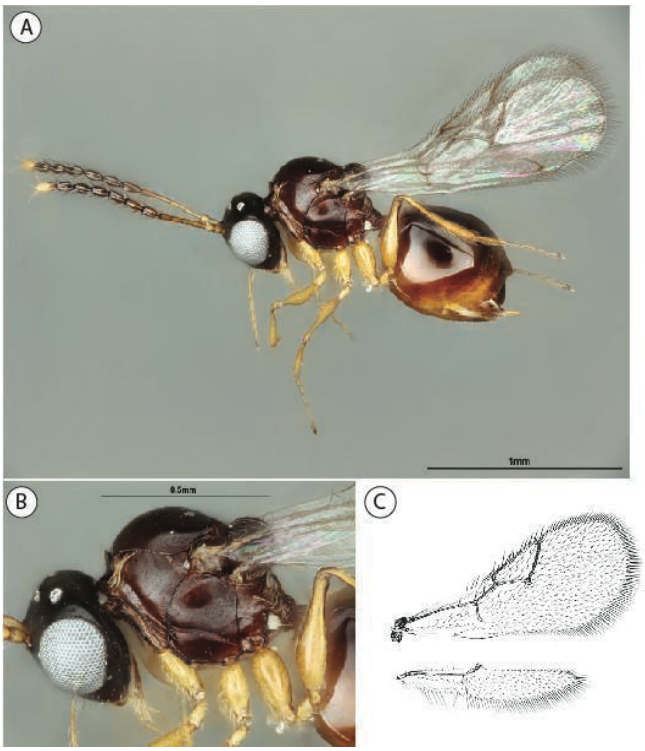

Figure 2. *Leptopilina malgretoutensis.* **(A)** Lateral view, **(B)** lateral view of mesosoma, and **(C)** wing vein pattern.

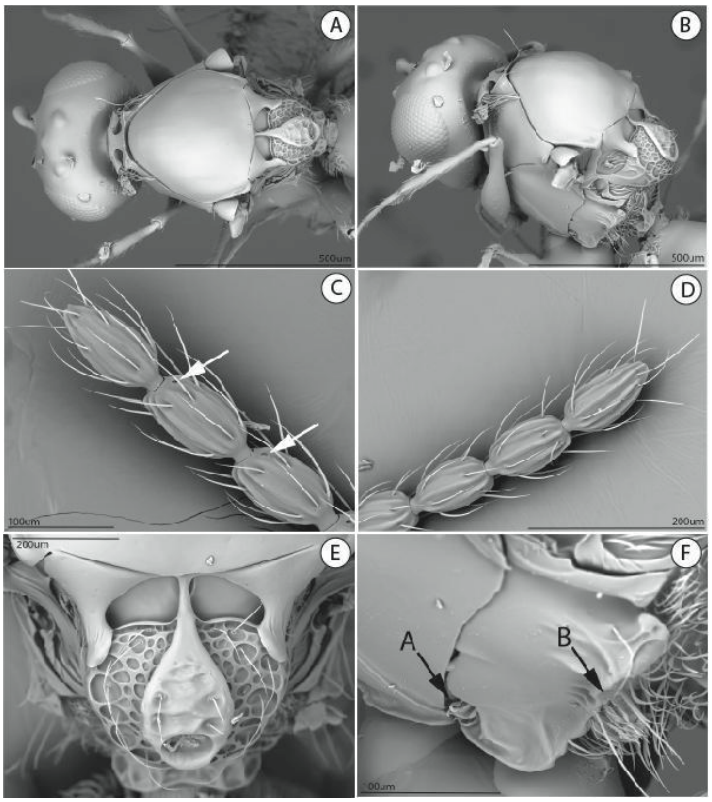

Figure 3. SEM images of *Leptopilina malgretoutensis.* **(A)** Top view of mesoscutum, **(B)** Lateral-posterior view of mesosoma, **(C)** campaniform sensillae, white arrow, compared to **(D)** no campaniform sensillae, **(E)** scutellum plate, and **(F)** metepimeron.

512 ***Leptopilina malgretoutensis* is highly virulent on *D. antillea* flies**

513 As noted extensively above, our laboratory cultures of *L. malgretoutensis* were collected on Saint Lucia.
514 This island is also the only reported location for the *Drosophila antillea* species of the dunni subgroup. To
515 our knowledge, the susceptibility of dunni group *Drosophila* to parasitoid wasps has not been previously
516 investigated. Thus, we wondered if the *D. antillea* flies would be susceptible, or if they were possibly
517 resistant, to infection by a wasp species that is also found on Saint Lucia. We allowed female wasps to
518 oviposit for 24 hours on larval cultures that were derived from isofemale lines of either *D. antillea* or *D.*
519 *willistoni* (that both originated from the STL3 collection site) and then determined the proportion of wasps
520 and flies that emerged from the infection vials. The results clearly indicated a high degree of virulence of
521 *L. malgretoutensis* on *D. antillea* (76.5% ± 5.6% wasp eclosion) relative to *D. willistoni* (20% ± 3.8% wasp
522 eclosion) as host species (Figure 4).

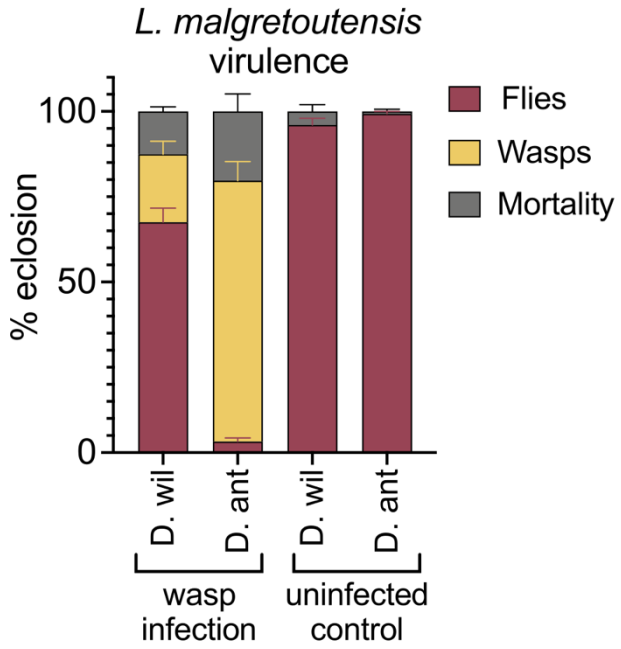

523

524 **Figure 4. *Leptopilina malgretoutensis* shows high virulence on a host fly species that is exclusive**
525 **to Saint Lucia.** Percentage of adult flies and wasps that eclosed from vials infected by *L.*
526 *malgretoutensis,* and from uninfected control vials. Mortality represents the percentage of larvae that did
527 not develop to adulthood. *L. mal.* is clearly more virulent on *Drosophila antillea* ("D. ant") hosts than on a
528 *Drosophila willistoni* ("D. wil") host strain that was also collected on Saint Lucia. Data are plotted as mean
529 ± SEM; n = 8 infection vials, n = 3 uninfected control vials.
530

531

532

533 ***Wolbachia* mediates obligate thelytokous parthenogenesis in *Leptopilina malgretoutensis***

534 While maintaining *L. malgretoutensis* wasp lines we noticed that the cultures were primarily female
535 (>95%). And, in one generation of passaging, the cultures became entirely female. Fearing that we would
536 lose the culture, we infected flies with these female wasps in an attempt to obtain haploid male offspring
537 that could be mated back to their mothers to obtain more diploid females. However, the cultures
538 generated by the virgin female wasps were again entirely female. This indicated that this species of wasp
539 was capable of asexually producing females (*i.e.*, thelytokous parthenogenesis). Furthermore, the
540 observation that males were rarely obtained in the cultures was unlikely to be strictly a consequence of
541 the wasps having especially high rates of fertilization (which gives rise to female offspring in
542 arrhenotokous, sexual, haplodiploids). In many parasitic wasp species, including a suite of other
543 *Leptopilina sp.*, thelytokous parthenogenesis is mediated by vertically transmitted bacterial symbionts
544 such as *Wolbachia* (α-proteobacteria: Rickettsiales) [47-49]. We tested for the presence of *Wolbachia*
545 infection by Western blot, targeting a *Wolbachia* specific protein and found that indeed the wasps were
546 infected with this microbe (Supplemental Figure S1).
547
548 To determine if a microbe was responsible for the asexual production of females, we used antibiotic
549 treatment with rifampicin to remove the infection and assess changes in the offspring sex ratio derived
550 from unmated females (Figure 5A). After treating unmated adult females (G_1) with rifampicin, they were
551 allowed to parasitize host larvae. Their broods (G_2) were almost entirely female (98.6% ± 2.6% female).
552 Critically, *Leptopilina* are largely proovigenic: all their eggs develop and mature during the pupal period
553 [50]. This means that symbiont-mediated effects are likely established much earlier, and treating adults is
554 "too late" (as has been seen in other wasps [51]). Thus, we performed a second generation of rifampicin
555 treatment: G_2 rifampicin-treated females produced offspring (F_0) that were almost all male (99.7% ± 0.3%
556 male), a clear indicator of symbiont-mediated parthenogenesis.
557
558 We attempted to generate a symbiont-free sexually reproducing line of wasps (Figure 5B) but were
559 unsuccessful. Specifically, symbiont depleted males and treated G_2 females were crossed to assess
560 sexual reproduction, but offspring continued to be almost all male (F_1-F_2, 91.2% ± 1.5% and 98.5% ±

561 0.6% male, respectively), indicating no sexual reproduction (Figure 5C). After antibiotic treatment was
562 discontinued, rare female progeny that were allowed to reproduce produced sex ratios that gradually
563 returned to being almost entirely female (F_3-F_4, 80% and 100% female, respectively), and unmated
564 females were again able to produce female offspring by parthenogenesis (F_5-F_6, 98.5% and 100%
565 female, respectively).

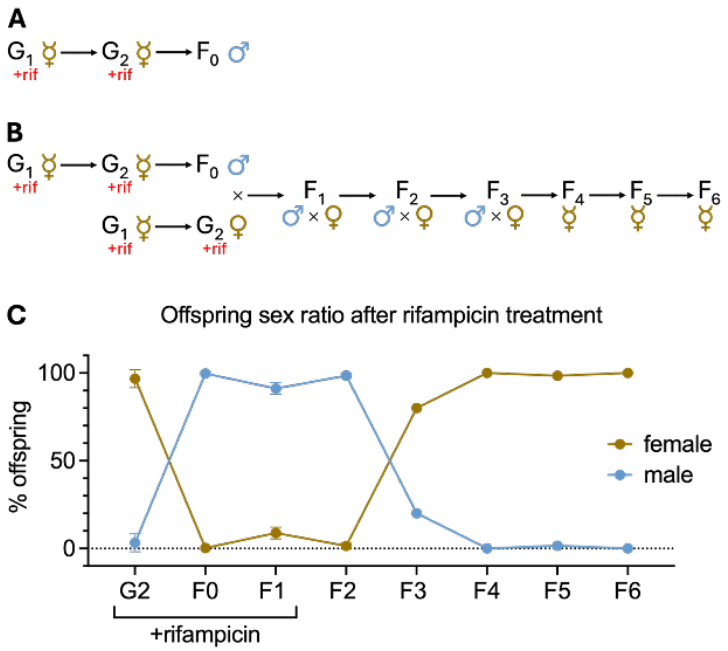

566
567 **Figure 5. *Leptopilina malgretoutensis* reproduces by symbiont-mediated thelytokous**
568 **parthenogenesis. (A)** Schematic depicting the production of male progeny after two generations of
569 antibiotic treatment ("+rif"), which supports the hypothesis of symbiont mediated parthenogenesis. **(B)**
570 Schematic of antibiotic treatment and crossing scheme to test for sexual reproduction after symbiont
571 depletion, and an attempt to generate a sexual, symbiont free strain. **(C)** Percentage of female and male
572 offspring in each generation. Data is plotted as mean ± SEM. For generations G_2 to F_2, n = 4-8 infection
573 vials; for generations F_3 to F_6, n = 1 infection vial.
574

575 ***Leptopilina malgretoutensis* genome sequencing and assembly**

576 We generated a genome assembly for *Leptopilina malgretoutensis* based on nanopore long read
577 sequencing (Table 1, Supplemental Tables S1-S3). The draft assembly with Flye leveraged all nanopore
578 reads longer than 5,000 bp (Supplemental Table S1) and generated 1,666 contigs totaling just over 1Gbp
579 in total length (Table 1; Supplemental Figure S2). The assembly was then polished with illumina short
580 reads: short-read mapping rates were very high (98.9% of reads mapped). After polishing, separating
581 cytoplasmic genomes, removing haplotigs, purging contaminants, and removing otherwise spurious
582 contigs, the ultimate nuclear genome assembly was 1,411 contigs and ~995Mbp in size with an N50 of

583 >1.8Mbp (Table 1). The longest contig in the assembly was close to 13Mbp in length. Assembly quality
584 was assessed with BUSCO. Just under 90% of the hymenopteran BUSCO proteins were complete,
585 similar to other assemblies in the genus (Table 2). We recovered two cytoplasmic genomes:
586 mitochondrion and *Wolbachia*. Additional low-coverage bacterial sequences that were purged from the
587 assembly belonged to typical associates of the fly food and microbiome (Supplemental Results in File S1
588 and Supplemental Table S3). No other symbionts were identified in the contigs (e.g., *Cardinium*,
589 *Spiroplasma,* etc [52-54]). Thus, we determine that *Wolbachia* is likely the cause of thelytokous
590 parthenogenesis.
591
592 **Table 1. Assembly statistics for *Leptopilina malgretoutensis***

Metric	**Draft**	**Ultimate**
Contigs	1,666	1,411
Length (bp)	1,004,830,435	994,936,849
Min length	499	5,452
Avg length	603,134	705,129
Max length	12,918,385	12,924,377
N50	1,831,405	1,832,545
%GC	29.85	29.75
BUSCO* (Hymenoptera)	C:89.3%[S:88.8%,D:0.5%], F:2.9%,M:7.8%,n:5991	C:89.7%[S:89.2%,D:0.5%],F:2.7%,M:7.6%,n:5991

593 *Standard BUSCO annotation: Complete BUSCOs (C) [Complete and single-copy BUSCOs (S),
594 Complete and duplicated BUSCOs (D)], Fragmented BUSCOs (F), Missing BUSCOs (M), Total BUSCO
595 groups searched (n)
596
597
598
599
600
601
602
603

604 **Table 2. Additional genomes used in comparative analyses.**

Species	Assembly Accession	Size (bp)	Protein Coding Genes	BUSCO* (Hymenoptera)
Leptopilina boulardi	ZJU_Lbou_2.1	354,804,354	13,647	C:91.4%[S:90.9%,D:0.5%], F:1.7%,M:6.9%,n:5991
Leptopilina clavipes	ASM185565v1	255,343,917	13,920	C:77.8%[S:77.3%,D:0.5%], F:7.3%,M:14.9%,n:5991
Leptopilina heterotoma	ASM1547642v1	484,694,486	14,450	C:91.1%[S:90.6%,D:0.5%], F:1.9%,M:7.0%,n:5991
Ganaspis kimorum[#]	GCA_037103525.1	1,025,447,244	20,567	C:89.4%[S:88.8%,D:0.6%], F:2.7%,M:7.9%,n:5991

605 * Standard BUSCO annotation: Complete BUSCOs (C) [Complete and single-copy BUSCOs (S),
606 Complete and duplicated BUSCOs (D)], Fragmented BUSCOs (F), Missing BUSCOs (M), Total
607 BUSCO groups searched (n). Hymenoptera dataset used.
608 [#] Previously '*Ganaspis* near *brasiliensis'* (including in genome report [55]), but recently re-assigned [6].
609

610 **Methylation**

611 We used a methyl-sensitive base-calling model to predict 5-methylcytosines in a CpG context. Across the
612 nuclear, mitochondrial, and *Wolbachia* genomes, fractional methylation was less than 1% (Genome:
613 0.600%, mitochondrion: 0.547%, *Wolbachia*: 0.598%). These estimates likely do not represent low levels
614 of true genomic methylation, rather, they are probably background noise due to error rates inherent to the
615 sequencing and base calling.

616

617 **Mitogenome**

618 We recovered a circular mitochondrial genome (14,490 bp; 20.6% GC; 3,562X sequencing coverage,
619 Figure 6, Supplemental Table S3). Using the barcoding sequence region from the mitochondrial genome,
620 plus representative sequences across the genus, we reconstructed a phylogeny of *Leptopilina sp.* (Figure
621 6A). *Leptopilina malgretoutensis* sequences were all identical, and formed a monophyletic group more
622 than 10% divergent from the next most closely related species in the dataset, further supporting its
623 designation as a new species. Importantly, *Leptopilina malgretoutensis* is sister to a clade within the
624 *Leptopilina* genus that contains all other species for which genome sequences are available (*Leptopilina*
625 *clavipes, Leptopilina boulardi,* and *Leptopilina heterotoma*). Annotation of the mitochondrial genome
626 revealed that gene order was largely conserved as compared to other *Leptopilina* mitochondria.

627 Additionally, we annotated the expected rRNAs and protein coding genes. However, insect mitochondrial
628 tRNAs are often difficult to annotate [56], and in *Leptopilina malgretoutensis* we were unable to find
629 tRNAs for asparagine (N), alanine (A), aspartic acid (D), pheylalanine (F), serine anticodon-1 (S1), and
630 arginine (R). Related to that, the region between the 3' end of the 16S rRNA (rrnL) and the 5' end of
631 *nad2*, was quite divergent as compared to *Leptopilina boulardi,* in which there is a cluster of tRNAs
632 (including D, F, S1, N, A, plus glutamic acid, glycine, and histidine). It is likely that divergence and/or
633 noncanonical tRNA structures, as is often the case in insect mitochondria, may be precluding a complete
634 annotation.

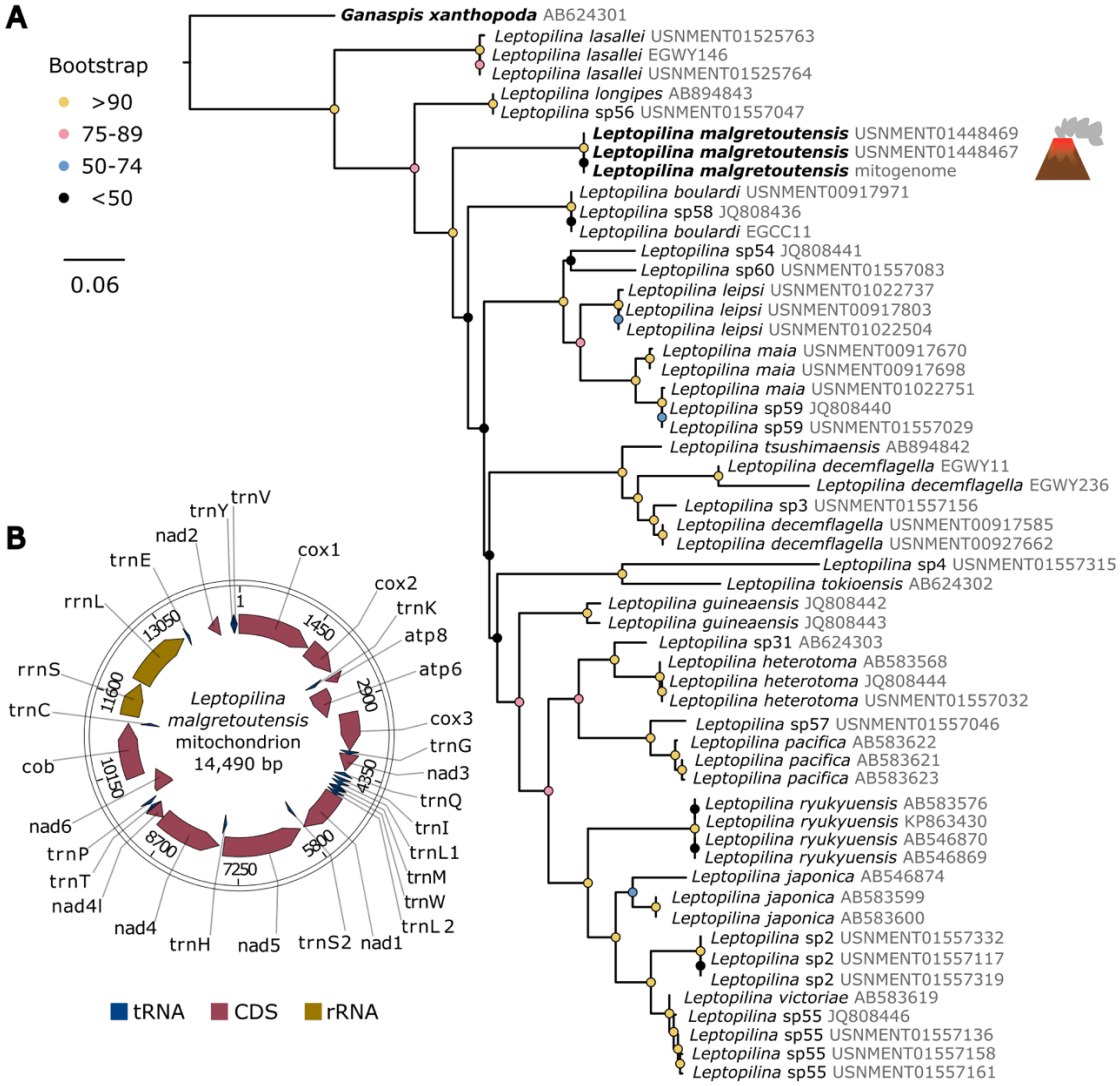

635
636 **Figure 6. Mitochondrial phylogeny and genome of *Leptopilina malgretoutensis*. (A)** Phylogenetic
637 reconstruction of *Leptopilina,* based on 480 nucleotides of Cox1, aligned to maintain codon position
638 relationships. Node colors indicate bootstrap support as indicated in legend. The three *Leptopilina*
639 *malgretoutensis* sequences are identical. The two other *L. malgretoutensis* sequences are from

640 previously barcoded STL6 specimens [3]. Sequences assigned to provisional species are indicated by
641 'sp' followed by a number, as per DROP database [3]. Accession numbers are in gray at the end of each
642 leaf label. **(B)** Map of the assembled mitochondrial genome and annotations.
643

644 **Gene Annotation**

645 Annotation of the repeat-masked *Leptopilina malgretoutensis* genome revealed 16,402 genes (Table 3),
646 which is in-line with annotations of closely related species (Table 2). To better understand genome
647 evolution, we clustered protein sequences (n=78,896 in total) of the four *Leptopilina* species plus
648 outgroup species *Ganaspis kimorum* [6, 55, 57-59]. As expected with a small set of closely related
649 species, we identified orthologs for most genes: 97.1% of the genes were clustered into 13,659
650 orthogroups, each of which contained 5.6 genes on average. 7,266 orthogroups contained genes from all
651 five species, and of those, 6,389 orthogroups were strictly single-copy. 1,077 orthogroups were species-
652 specific and only contained in-paralogs.
653

654 **Table 3. Annotation metrics for the *Leptopilina malgretoutensis* genome.**

Metric	Value*
Number of genes	16,402
Number of mRNAs	18,165
Number of exons	97,163
Number of introns	78,998
Mean mRNAs per gene	1.1
Mean exons per mRNA	5.3
Total gene length	158,352,048 bp
Longest gene	235,629 bp
Mean gene length	9,654 bp
Longest CDS	76,353 bp
Mean CDS length	1,541 bp
Longest exon	16,278 bp
Mean exon length	288 bp

655 *Base pairs = bp
656

657 **Repetitive elements**

658 Given the larger than expected size of the *Leptopilina malgretoutensis* genome relative to other
659 *Leptopilina* species, we analyzed the repeat content of the assembly using a *de novo* repeat identification
660 pipeline. 66.81% of the nearly 1Gbp genome assembly was identified as repetitive (Figure 7,
661 Supplementary Table S4). Retroelements and DNA transposons only constituted 9.57% and 5.09% of the
662 length of the assembly, respectively. The majority of the repeat content (48.97% of the assembly) was
663 categorized as unclassified repetitive elements. To determine if this large repetitive fraction was unique to
664 *Leptopilina malgretoutensis* we ran the same *de novo* repeat identification pipeline on the three other
665 *Leptopilina* species with genome assemblies available, plus an outgroup from a closely related genus,
666 *Ganaspis kimorum* (Supplemental Table S4). Indeed, the other *Leptopilina* species were less repeat
667 dense with 35.40%, 48.01%, and 57.27% repeat content for *L. clavipes, boulardi, and heterotoma,*
668 respectively. Similar to *Leptopilina malgretoutensis*, the majority of these repetitive elements were
669 unclassified. In fact, the overall size and makeup of the *Leptopilina malgretoutensis* genome was much
670 more similar to the outgroup *Ganaspis kimorum* (Figure 7A,B). However, the *Ganaspis kimorum* and
671 *Leptopilina malgretoutensis* genomes contained approximately double the amount of non-repetitive
672 genome as compared to the other *Leptopilina* (black bars in Figure 7B). Thus, while *Leptopilina*
673 *malgretoutensis* had the largest repetitive content in the genus (both by total length and percentage),
674 repeat content alone does not completely explain the overall difference in genome size relative to the
675 other congenerics.
676
677 To understand the large differences in repeat content across the *Leptopilina* genomes, we performed an
678 all-versus-all analysis in which we mapped each species' repeat library to all other species' genomes
679 (Figure 7C). Then we determined how many of the unique repeat families were present to infer if there
680 was simply a difference in the number of repeat occurrences (e.g., family size), or, if entire repeat families
681 had been gained or lost across the clade. The most repeat dense genomes, *Ganaspis kimorum* and
682 *Leptopilina malgretoutensis*, contained 3,563 and 4,002 repeat families respectively, likely indicating a
683 gain of repeats in the *Leptopilina* common ancestor. Accordingly, while 84.1% of the *Ganaspis kimorum*
684 repeat families occur in the *Leptopilina malgretoutensis* genome, only 82.5% of the *Leptopilina*

685 *malgretoutensis* repeat families occur in *Ganaspis kimorum*. There appears to have been a large loss of
686 repeat families in the ancestor of the clade containing *L. boulardi*, *L. heterotoma*, and *L. clavipes*, and
687 additional loss in the lineage leading to *L. clavipes*. These genomes contained 2,727, 2,742, and 1,718
688 families respectively, and between 88-91% of these families were found in *L. malgretoutensis*.
689 Furthermore, while only 78-80% of the *L. malgretoutensis* repeats were identified in these other
690 *Leptopilina* genomes, an even lower percentage of the *Ganaspis kimorum* repeats were present (73.3-
691 77.5%). Finally, the comparisons within the clade of *L. boulardi*, *L. heterotoma*, and *L. clavipes*, indicate
692 high levels of shared repeats (85.8-93.9%). All together, these data indicate that (1) the ancestor of the
693 four *Leptopilina* species here acquired repetitive elements that are not present in *Ganaspis kimorum*, (2)
694 many of the repeats have since been lost in *L. boulardi*, *L. heterotoma*, and especially in *L. clavipes*.
695

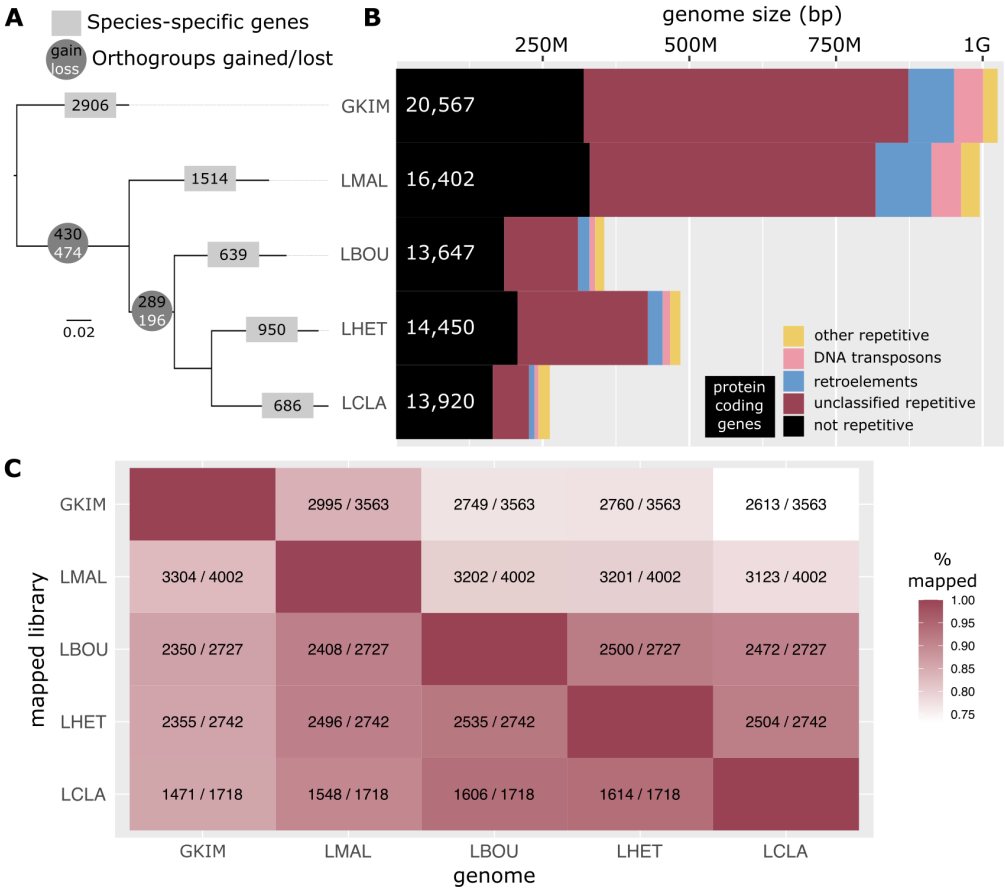

696
697 **Figure 7. Evolution of *Leptopilina* genomes. (A)** Species tree inferred by OrthoFinder, rooted on
698 outgroup, *Ganaspis kimorum*. Phylogeny is annotated with (1) the number of species-specific genes (gray
699 boxes), which include both singletons, and species-specific orthogroups, and (2) inferred gains and
700 losses of orthogroups. "Gained" orthogroups are those that are unique to and present in all taxa within the
701 clade, and "lost" orthogroups are present in all the outgroups, but none of the ingroups. **(B)** Genome

content of each representative assembly. **(C)** All-verus-all comparison of repetitive elements. Libraries of the *de novo* identified repeats from each species were mapped to all other genomes, and the number of unique repeat families recovered in each comparison is indicated within each box in the heat map (number of families identified in "genome"/number of unique families in "library").

***Wolbachia* Strain *w*Lmal**

We identified a circular *Wolbachia* genome in our assembly, hereinafter strain "*w*Lmal" (Table 4). A single contig was sequenced at 344X coverage and blast results from blobtools revealed similarity to *Wolbachia* strain *w*Ha from *Drosophila simulans* across most of the contig. BUSCO genome completeness metrics were very high, with 99.2% of Rickettsiales BUSCOs present in single copy (Table 4). Phylogenetic reconstruction based on core single-copy orthologs revealed that *w*Lmal is closely related to *Drosophila* infecting *Wolbachia* strains (e.g., *w*Mel, *w*Ha*, w*Ri, *w*Au) in *Wolbachia* Supergroup A (Figure 8A). This is notable not only due to the host-parasitoid relationship of *Leptopilina* and *Drosophila*, but also because the parthenogenesis-inducing "*w*Lcla" strain from *Leptopilina clavipes* is quite divergent, and nested within a different major *Wolbachia* clade: Supergroup B [60, 61]. The size (~1.2Mbp) and coding content of the *w*Lmal genome is quite typical of an insect-infecting *Wolbachia* strain [62, 63] (Figure 8B, Table 4). Two putative prophage regions were identified. The first (1,00,3471 bp - 1,051,238 bp) is partial and is likely remnants of a *Wolbachia* "WO" prophage. This prophage region contains some phage structural elements (primarily proteins for the tail) and what looks to be part of a "Eukaryotic Association Module" (EAM), a region associated with WO phages which often contains proteins for manipulating host reproduction and cell biology [64]. The second predicted prophage region (824,983 bp - 864,973 bp) appears much more degenerate and only has a few remaining open reading frames encoding for phage proteins.

We searched for the two recently identified putative parthenogenesis-inducing effector proteins, *pifA* and *pifB,* which are found in the parthenogenesis inducing strains *w*Lcla and *w*Tpre [60]. *pifA* is also present in the PI-*Wolbachia* infecting *Encarisa formosa* (designated *"piff"* in that strain) [65]. We identified two identical copies of *pifB*, but did not find evidence for *pifA* in *w*Lmal (Supplemental File S1). Closer inspection revealed that the *pifB* copies are in opposite orientations, and one copy of *pifB* is surrounded by insertion elements and is just downstream of a putative *hin* DNA invertase, likely from the WO phage.

732 We also queried the *w*Lmal genome for a suite of other notable *Wolbachia* proteins and identified other
733 putative or confirmed effector proteins. Surprisingly, these included the genes *cifA* and *cifB* (here,
734 specifically "type I" or *cid*-type [66] which cause an entirely different host reproductive phenotype: the
735 conditional sperm-egg incompatibility known as cytoplasmic incompatibility (CI).
736

737 **Table 4. *Wolbachia* strain *w*Lmal genome assembly and annotation.**

Metric	***w*Lmal**
Contigs	1
Length (bp)	1,198,858
%GC	35.1
BUSCO* (Rickettsiales)	C:99.2%[S:99.2%,D:0.0%], F:0.3%,M:0.5%,n:364
CDS	1,356
rRNAs	3
tRNAs	34

738 *Standard BUSCO annotation: Complete BUSCOs (C) [Complete and single-copy BUSCOs (S),
739 Complete and duplicated BUSCOs (D)], Fragmented BUSCOs (F), Missing BUSCOs (M), Total BUSCO
740 groups searched (n)

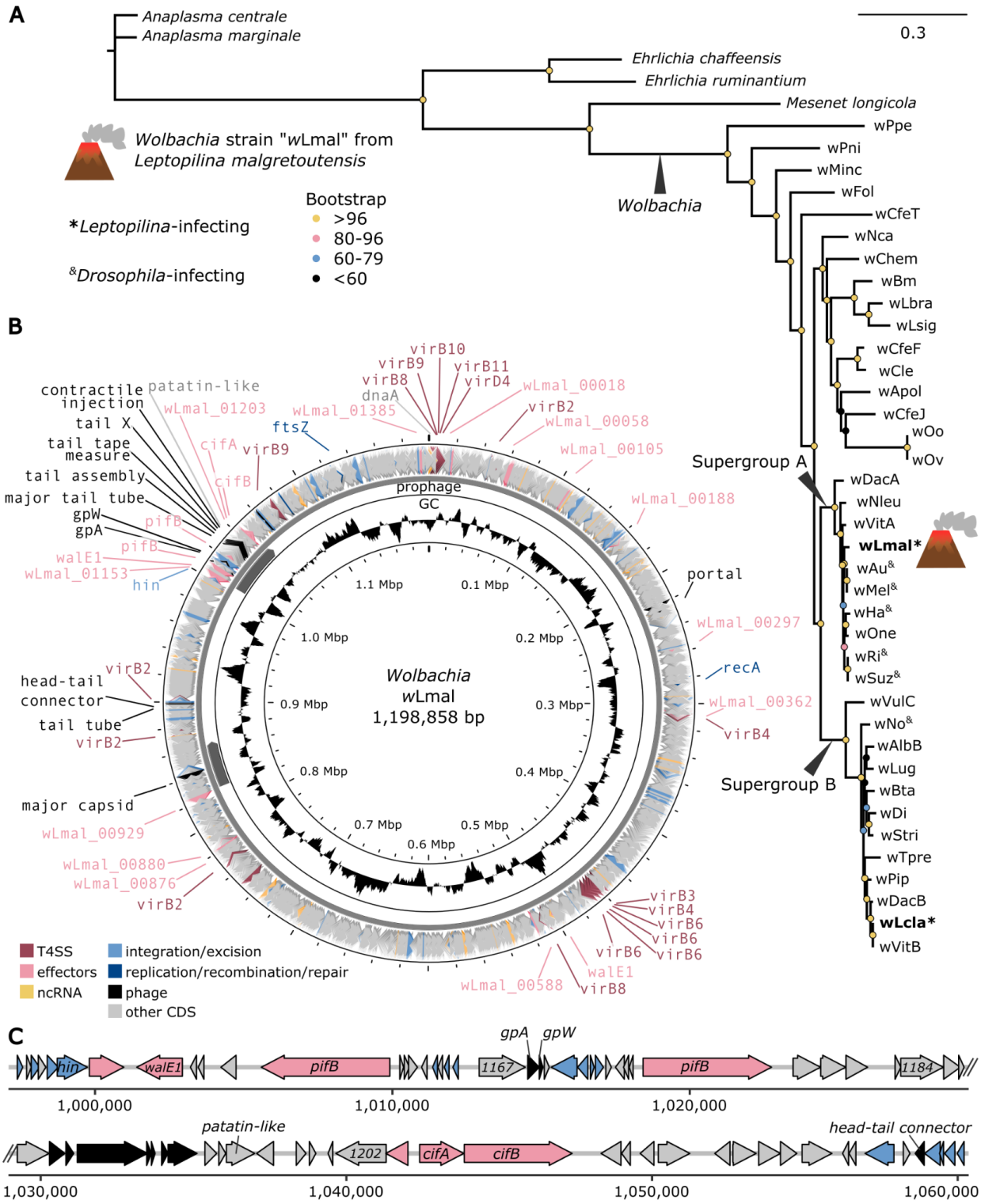

Figure 8. *Wolbachia* strain *w*Lmal. (A) Phylogenetic relationships of *Wolbachia* strains and Rickettsiales relatives based on 127 core single-copy orthologs. **(B)** Map of the complete *w*Lmal genome. Each concentric circle is annotated with a different set of genomic information. The innermost circle is annotated with a basepair marker, the second circle indicates GC content, the third circle indicates prophage regions identified by VirSorter, and the outermost circle shows the coding regions of the genome. Abbreviations: Type IV Secretion system (T4SS), noncoding RNA (ncRNA), coding sequences

(CDS). Putative effector proteins are indicated with the gene name where possible, otherwise the wLmal CDS number is indicated and the *w*Mel homologs can be found in Supplemental Table S5. **(C)** Gene models in the prophage region containing remnant WO phage structural proteins and a suite of effector proteins homologs. Notably the two *pifB* coding sequences are present in an inverted repeat. Open reading frames labeled with numbers (e.g., 1167) are gene annotation IDs, provided to benchmark the region.

Historical specimens of *Leptopilina malgretoutensis*

As noted above, our Saint Lucian specimens matched previously undescribed *Leptopilina* collected from the Caribbean in the 1980's (specimens USNMENT01025775-USNMENT01025782). Specifically, those *Leptopilina* (n=16, all female) were collected in 1982 and 1983 from Grande Terre, Guadeloupe (~270 km from our collection site on Saint Lucia), some of which were used to initiate a now extinct colony, "PB10-5". The PB10-5 wasps were previously characterized as an undescribed species nested within an early-branching *Leptopilina* lineage, in the same clade as *Leptopilina longipes* [67, 68]. Our COI phylogenetic reconstruction of *Leptopilina* recapitulated these relationships (Figure 6A). In addition to all the collected Guadeloupe wasps being female, Yves Carton's notes indicated "*[the PB10-5 colony] emerged only females: we can conclude that this species is parthenogenetic.*" In summary, our data indicate that *L. malgretoutensis* was previously collected ~40 years ago on the neighboring island of Guadeloupe and also reproduced via thelytokous parthenogenesis.

DISCUSSION

Our study represents a comprehensive description of *Leptopilina malgretoutensis*, the first recorded parasitoid of *dunni* group *Drosophila* from their native range. By integrating classic taxonomy and systematics approaches with genomics and experimental biology, we were able to generate a more comprehensive view of the biology and evolution of this new species. Furthermore, historical records and museum specimens enabled the discovery that asexually reproducing *Leptopilina malgretoutensis* have also been found on another island in the Antilles. This work represents one of a limited number of studies in which description of a new metazoan species is coupled with genome sequencing [69-73]. Indeed, this is the fifth such example in insects [74-77], wherein body size often precludes whole genome sequencing of holotypes.

779 Despite the interest in speciation patterns of the *dunni* group *Drosophila*, the proximal ecological or
780 evolutionary mechanisms driving morphological and species diversity in this group remain unresolved.
781 One study found elevated nonsynonymous substitution rates in the pigmentation gene *yellow* in two
782 members of this group [78]. This is consistent with selection for pigmentation diversity, but no studies
783 have yet identified the selective agent responsible for this pattern. Importantly, melanization is a process
784 in many insect lineages that is critical in both the development of cuticle pigmentation as well as in
785 immune responses that occur during encapsulation of foreign pathogens [79]. In *Drosophila*, melanization
786 is a well-studied response to infection by eukaryotic parasites (including *Leptopilina*) and is linked to the
787 same genetic pathways as pigmentation production [80-82]. In one study in *Drosophila falleni*, selection
788 for a reduced number of abdominal spots resulted in higher infection rates by a parasitic nematode [83].
789 In other insects there are similar links between the levels or patterns of cuticular melanization and
790 resistance to parasites [84-89]. As such, it has been postulated that *Drosophila* abdominal coloration may
791 vary in some systems primarily due to selection by parasitism [90, 91], but direct evidence for this is
792 lacking.
793
794 Since adult flies of the *D. antillea* species are among the more highly pigmented flies of the *dunni* group,
795 we were interested in the possibility that they might be particularly resistant to infection by endemic
796 parasitoids. However, we instead found the opposite. *L. malgretoutensis* wasps are highly virulent on *D.*
797 *antillea* hosts. This observation could indicate that *L. malgretoutensis* is a relatively recent colonizer of
798 Saint Lucia and that *D. antillea* has not had sufficient time to evolve resistance. In contrast, *L.*
799 *malgretoutensis* was less effective at using *D. willistoni* as a host. Our findings open the door to future
800 studies to explore the potential mechanism of *L. malgretoutensis* virulence on flies of the *dunni* group as
801 well as the potential mechanisms of resistance for *D. willistoni.* It will also be of interest to test the
802 virulence of *L. malgretoutensis* on other species from the *dunni* group as well as how virulence tracks with
803 island of origin of the wasp. For example, are *L. malgretoutensis* wasps as effective when infecting *dunni*
804 group flies that are native to other islands of the Antilles chain? Are *L. malgretoutensis* wasps that
805 originate from Guadeloupe as virulent on *D. antillea*? Indeed, the island of Guadeloupe where Carton
806 collected *L. malgretoutensis* is home to the dunni group fly *Drosophila arawakana.* It would be of interest

807 to know how the virulence of Guadeloupian wasps relates to Saint Lucian wasps on fly species from the
808 various islands.
809
810 The island biogeography of *L. malgretoutensis* may also play a role in the evolution of their reproductive
811 mode. Our antibiotic curing experiments indicated that our *L. malgretoutensis* colony derived from Saint
812 Lucia is unable to revert to sexual reproduction. The inability to restore sex is a strong indicator of a so-
813 called "virginity mutation", which is well described in several other wasp species with symbiont-mediated
814 parthenogenesis [58, 92-97]. There are multiple hypotheses for the evolutionary pressures that lead to
815 virginity mutations [49, 92, 98, 99], but in brief, they are mutations that result in the decay or loss of
816 sexual function, to the point that the animal becomes reliant upon the PI symbiont for the production of
817 female offspring. Related to this, it is notable that the colony of *L. malgretoutensis* derived from
818 Guadeloupe collections in the 1980s were all female. However, we do not know if this PB10-5 colony was
819 (a) infected with *Wolbachia*, (b) asexual because of *Wolbachia*, or (c) obligately asexual (i.e., unable to
820 revert to a sexual mode). Indeed, some other populations of parasitic wasps with PI *Wolbachia* have
821 significant within-species polymorphism and vary in which *Wolbachia* strain they have, if they are
822 asexually reproducing, and if they have a so-called virginity mutation [49, 100]. Thus, it may be that
823 populations of *L. malgretoutensis* on different islands vary in whether they are sexually reproducing, and if
824 asexual reproduction is fixed or reversible. Notably, asexual reproduction across many taxa appears to be
825 more common on islands [101, 102], and thus *L. malgretoutensis* in the Lesser Antilles may provide a
826 tractable system to understand the evolution of reproductive mode in the context of biogeography.
827
828 While there are many other examples of species with virginity mutations, our findings are quite unusual in
829 that the *Wolbachia* genome here also contains what appears to be functional genes for inducing
830 cytoplasmic incompatibility (CI). Paradoxically, the CI phenotype only manifests with sexual reproduction:
831 males with CI *Wolbachia*-modified sperm cause embryonic lethality in embryos derived from females
832 without a compatible *Wolbachia* strain [66]. We have several hypotheses for why these *Wolbachia*
833 encode for CI loci despite inducing parthenogenesis. First, the *cif* loci may have undergone some form of
834 neofunctionalization: perhaps these proteins are no longer involved in sperm-egg incompatibility as in CI

835 but are impacting other host processes. Alternatively, it might be that the transition to parthenogenesis is
836 more recent, and CI is no longer under selection. Perhaps the *cifs* are en route to be eliminated from the
837 genome in the future. “Recent” is of course difficult to determine quantitatively, especially in island
838 systems where there are often strong bottlenecks that can drive rapid evolution [103]. Finally, it might be
839 that if the PI phenotype has lower penetrance and occasional males are produced. These males might
840 mate with incompatible conspecifics (that either have no *Wolbachia* or an incompatible strain) and induce
841 CI, perhaps reducing competition for the asexual matriline. However, we see two issues with this
842 scenario. First, lower penetrance of PI phenotypes is typically due to the loss of *Wolbachia* (e.g., due to
843 higher temperatures, or in the lab, antibiotics), which leads to the production of males. In this case, the
844 occasional males produced by PI mothers might not have sufficient *Wolbachia* to induce CI. Second,
845 because the PI females transmitting *Wolbachia* to the next generation would never need to rescue CI,
846 there would be no selection pressure to maintain CI function.
847
848 Despite the peculiarity of a PI *Wolbachia* strain encoding for CI genes, all four loci associated with host
849 reproductive manipulation (*cifA, cifB,* and two copies of *pifB*) are found in the EAM of WO: a classic
850 signature of *Wolbachia* genomes and reproductive effector proteins. The multiple identical *pifB* copies,
851 genes for CI in combination with a clear *Wolbachia*-mediated PI phenotype, and evidence for multiple
852 prophage infections all point towards recent dynamism in the *w*Lmal genome. Many *Wolbachia* genes
853 mediating host reproductive switches are horizontally acquired from other *Wolbachia* strains, likely due to
854 the WO phage [64, 104]. For this reason, it was not surprising that the two PI *Wolbachia* strains from
855 *Leptopilina* both encoded for PifB proteins, despite the strains belonging to different clades. In contrast,
856 we did not find any evidence in *w*Lmal for the PifA protein, a *transformer* mimic that interacts with the
857 sexual differentiation pathway [60, 65]. Importantly however, we do not know the exact mechanism of
858 parthenogenesis induction employed by *w*Lmal (e.g., one versus two step, apomixis versus gamete
859 duplication, etc [105]). And, given the diversity of PI mechanisms found across *Wolbachia* [49] it is quite
860 possible that *w*Lcla and *w*Lmal are not using precisely the same toolset. Closer inspection of meiosis and
861 early embryonic mitoses in *L. malgretoutensis* will be key to understanding how *w*Lmal causes PI, and
862 what the role of PifB, or other proteins, might be in this process. Altogether, the description of *L.*

863 *malgretoutensis* and its reproductive biology will enable future explorations of host-parasitoid and host-
864 symbiont interactions, especially in the context of speciation.
865
866 In summary, this study provides a clear example of how descriptive work in under-studied species can
867 lead to novel discoveries across a broad set of biological disciplines. Insects generally, but especially
868 parasitic Hymenoptera, are under described [5]. Furthermore, of the described parasitic hymenopterans,
869 a significant majority lack biological information such as host associations and ecology. Here,
870 identification of a new species of parasitoid has provided a unique view into the intricate co-evolution of
871 host insect, parasitoid, and *Wolbachia* symbiont, with dynamic interactions between genomic evolution,
872 virulence, and reproductive ecology. We hope our work inspires more integration of descriptions of new
873 species coupled with investigations into novel aspects of their biology.
874
875 **DATA AVAILABILITY**
876 BioProject: PRJNA1150626
877 *L. malgretoutensis* BioSample: SAMN43291974
878 *w*Lmal BioSample: SAMN43291989
879 Oxford Nanopore Technologies Long Reads (all, including <5kbp): SRR30339708
880 WGS Illumina Reads: SRR30339709
881 RNA-seq Illumina Reads: SRR30339707
882 *L. malgretoutensis* Mitochondrial Genome: #Accession Forthcoming
883 *w*Lmal *Wolbachia* Genome: CP185405.1
884 *L. malgretoutensis* Nuclear Genome Assembly: This Whole Genome Shotgun project has been deposited
885 at DDBJ/ENA/GenBank under the accession JBMIRX000000000. The version described in this paper is
886 version JBMIRX010000000.
887
888 Supplemental File S1 contains:
889 Supplemental Text
890 Figure S1. Western Blot for *Wolbachia* detection.

Figure S2. Draft assembly snail plot and blob plot.

Supplemental Tables are provided in an excel file where each sheet corresponds to a different table number:

Table S1. Passed reads statistics.

Table S2. All draft assembly contigs statistics, including BlobTools annotations.

Table S3. Purged contigs.

Table S4. Repeat annotations.

Table S5. *Wolbachia* protein queries.

Table S6. wLmal phage annotation.

ACKNOWLEDGEMENTS

The research expedition of the sailing vessel Sea Salt was conceived in conversations with W. Daniel Tracey Sr. (now deceased), and we dedicate this study to his memory. We are very thankful to Amalia Rowan the first mate on the Sea Salt without whose assistance our collection expedition could not have taken place. We are thankful for Dr. Hannah Romain (Saint Lucia Ministry of Agriculture) for granting permission to collect insects on Saint Lucia. We are also thankful to Michael Gerth for making the WHOP pipeline available and to Keith Hopper for sharing the *Ganaspis* assembly prior to its release. Research reported in this publication was supported by the National Institute of General Medical Sciences of the National Institutes of Health under award number R35GM150991 to ARIL, the National Institute of Food and Agriculture Predoctoral Fellowship to LCF (NIFA 2023-67034-40496), and the Linda and Jack Gill Institute for Neuroscience Research Stipend to WDT. Mention of trade names or commercial products in this publication is solely for the purpose of providing specific information and does not imply recommendation or endorsement by the USDA. USDA is an equal opportunity provider and employer.

CONFLICTS OF INTEREST

MKD works for Oxford Nanopore Technologies.

CITATIONS

1. Karvonen A, Seehausen O. The role of parasitism in adaptive radiations—when might parasites promote and when might they constrain ecological speciation? International Journal of Ecology. 2012;2012(1):280169.

2. Nyman T, Bokma F, Kopelke J-P. Reciprocal diversification in a complex plant-herbivore-parasitoid food web. BMC Biol. 2007;5:1-9.

3. Lue CH, Buffington ML, Scheffer S, Lewis M, Elliott TA, Lindsey AR, et al. DROP: Molecular voucher database for identification of *Drosophila* parasitoids. Molecular Ecology Resources. 2021;21(7):2437-54.

4. Saunders TE, Ward DF. Variation in the diversity and richness of parasitoid wasps based on sampling effort. PeerJ. 2018;6:e4642.

5. Forbes AA, Bagley RK, Beer MA, Hippee AC, Widmayer HA. Quantifying the unquantifiable: why Hymenoptera, not Coleoptera, is the most speciose animal order. BMC Ecol. 2018;18:1-11.

6. Sosa-Calvo J, Forshage M, Buffington ML. Circumscription of the *Ganaspis brasiliensis* (Ihering, 1905) species complex (Hymenoptera, Figitidae), and the description of two new species parasitizing the spotted wing drosophila, *Drosophila suzukii* Matsumura, 1931 (Diptera, Drosophilidae). J Hymenoptera Res. 2024;97:441-70.

7. Coyne JA, Orr HA. Speciation: a catalogue and critique of species concepts. Philosophy of Biology: An Anthology. 2004:272-92.

8. Carson HL, Templeton AR. Genetic revolutions in relation to speciation phenomena: the founding of new populations. Annu Rev Ecol Syst. 1984:97-131.

9. Kaneshiro K, Gillespie R, Carson H. Chromosomes and male genitalia of Hawaiian *Drosophila*: tools for interpreting phylogeny and geography. Hawaiian Biogeography: Evolution on a hot spot archipelago. 1995:57-71.

10. O'Grady P, DeSalle R. Hawaiian *Drosophila* as an evolutionary model clade: days of future past. Bioessays. 2018;40(5):1700246.

11. Dworkin I, Jones CD. Genetic changes accompanying the evolution of host specialization in *Drosophila sechellia*. Genetics. 2009;181(2):721-36.

12. Hollocher H. Island hopping in *Drosophila*: patterns and processes. Philosophical Transactions of the Royal Society of London Series B: Biological Sciences. 1996;351(1341):735-43.

13. Heed WB, Krishnamurthy NB. Genetic studies on the cardini group of *Drosophila* in the West Indies. Univ Texas Publ. 1959;5914:155-79.

14. Hollocher H, Hatcher JL, Dyreson EG. Genetic and developmental analysis of abdominal pigmentation differences across species in the *Drosophila dunni* subgroup. Evolution. 2000;54(6):2057-71.

15. Lue C-H, Driskell AC, Leips J, Buffington ML. Review of the genus *Leptopilina* (Hymenoptera, Cynipoidea, Figitidae, Eucoilinae) from the Eastern United States, including three newly described species. J Hymenoptera Res. 2016;(53).

958 16. Stacconi MVR, Buffington M, Daane KM, Dalton DT, Grassi A, Kaçar G, et al. Host stage
959 preference, efficacy and fecundity of parasitoids attacking *Drosophila suzukii* in newly invaded areas. Biol
960 Control. 2015;84:28-35.

961 17. Abram PK, Franklin MT, Hueppelsheuser T, Carrillo J, Grove E, Eraso P, et al. Adventive larval
962 parasitoids reconstruct their close association with spotted-wing drosophila in the invaded North
963 American range. Environ Entomol. 2022;51(4):670-8.

964 18. Newton IL, Savytskyy O, Sheehan KB. *Wolbachia* utilize host actin for efficient maternal
965 transmission in *Drosophila melanogaster*. PLoS Path. 2015;11(4):e1004798. doi:
966 10.1371/journal.ppat.1004798. PubMed PMID: 25906062; PubMed Central PMCID: PMCPMC4408098.

967 19. Lindsey AR, Tennessen JM, Gelaw MA, Jones MW, Parish AJ, Newton IL, et al. The intracellular
968 symbiont *Wolbachia* alters *Drosophila* development and metabolism to buffer against nutritional stress.
969 bioRxiv. 2023.

970 20. Fricke LC, Lindsey AR. Examining *Wolbachia*-Induced Parthenogenesis in Hymenoptera.
971 *Wolbachia*: Methods and Protocols: Springer; 2024. p. 55-68.

972 21. Shen W, Le S, Li Y, Hu F. SeqKit: a cross-platform and ultrafast toolkit for FASTA/Q file
973 manipulation. PLoS One. 2016;11(10):e0163962.

974 22. Kolmogorov M, Yuan J, Lin Y, Pevzner PA. Assembly of long, error-prone reads using repeat
975 graphs. Nat Biotechnol. 2019;37(5):540-6.

976 23. Roach MJ, Schmidt SA, Borneman AR. Purge Haplotigs: allelic contig reassignment for third-gen
977 diploid genome assemblies. BMC Bioinformatics. 2018;19(1):1-10.

978 24. Li H. Aligning sequence reads, clone sequences and assembly contigs with BWA-MEM. arXiv
979 preprint arXiv:13033997. 2013.

980 25. Li H, Handsaker B, Wysoker A, Fennell T, Ruan J, Homer N, et al. The Sequence Alignment/Map
981 format and SAMtools. Bioinformatics. 2009;25(16):2078-9. doi: 10.1093/bioinformatics/btp352.

982 26. Challis R, Richards E, Rajan J, Cochrane G, Blaxter M. BlobToolKit–interactive quality
983 assessment of genome assemblies. G3: Genes, Genomes, Genetics. 2020;10(4):1361-74. PubMed
984 Central PMCID: PMCPMC7144090.

985 27. Simão FA, Waterhouse RM, Ioannidis P, Kriventseva EV, Zdobnov EM. BUSCO: Assessing
986 genome assembly and annotation completeness with single-copy orthologs. Bioinformatics. 2015. doi:
987 10.1093/bioinformatics/btv351.

988 28. Astashyn A, Tvedte ES, Sweeney D, Sapojnikov V, Bouk N, Joukov V, et al. Rapid and sensitive
989 detection of genome contamination at scale with FCS-GX. Genome Biol. 2024;25(1):60.

990 29. Bernt M, Donath A, Jühling F, Externbrink F, Florentz C, Fritzsch G, et al. MITOS: improved de
991 novo metazoan mitochondrial genome annotation. Mol Phylogen Evol. 2013;69(2):313-9.

992 30. Wanner N, Larsen PA, McLain A, Faulk C. The mitochondrial genome and Epigenome of the
993 Golden lion Tamarin from fecal DNA using Nanopore adaptive sequencing. BMC Genomics. 2021;22:1-
994 11.

995 31. Katoh K, Standley DM. MAFFT multiple sequence alignment software version 7: improvements in
996 performance and usability. Mol Biol Evol. 2013;30(4):772-80. doi: 10.1093/molbev/mst010.

997 32. Nguyen L-T, Schmidt HA, Von Haeseler A, Minh BQ. IQ-TREE: a fast and effective stochastic
998 algorithm for estimating maximum-likelihood phylogenies. Mol Biol Evol. 2015;32(1):268-74.

999 33. Flynn JM, Hubley R, Goubert C, Rosen J, Clark AG, Feschotte C, et al. RepeatModeler2 for
1000 automated genomic discovery of transposable element families. Proc Natl Acad Sci. 2020;117(17):9451-
1001 7.

1002 34. Storer J, Hubley R, Rosen J, Wheeler TJ, Smit AF. The Dfam community resource of
1003 transposable element families, sequence models, and genome annotations. Mobile DNA. 2021;12:1-14.

1004 35. Keilwagen J, Hartung F, Grau J. GeMoMa: homology-based gene prediction utilizing intron
1005 position conservation and RNA-seq data. Gene Prediction: Methods and Protocols. 2019:161-77.

1006 36. Dobin A, Gingeras TR. Mapping RNA-seq reads with STAR. Current Protocols in Bioinformatics.
1007 2015;51(1):11.4. 1-.4. 9.

1008 37. Emms DM, Kelly S. OrthoFinder: phylogenetic orthology inference for comparative genomics.
1009 Genome Biol. 2019;20:1-14.

1010 38. Gerth M. WHOP (v0.1). Zenodo. 2023. doi: https://doi.org/10.5281/zenodo.8343898.

1011 39. Seemann T. Prokka: rapid prokaryotic genome annotation. Bioinformatics. 2014;30(14):2068-9.

1012 40. Bruen T, Bruen T. PhiPack: PHI test and other tests of recombination. McGill University,
1013 Montreal, Quebec. 2005:1-8.

1014 41. Grant JR, Enns E, Marinier E, Mandal A, Herman EK, Chen C-y, et al. Proksee: in-depth
1015 characterization and visualization of bacterial genomes. Nucleic Acids Res. 2023;51(W1):W484-W92.

1016 42. Guo J, Bolduc B, Zayed AA, Varsani A, Dominguez-Huerta G, Delmont TO, et al. VirSorter2: a
1017 multi-classifier, expert-guided approach to detect diverse DNA and RNA viruses. Microbiome. 2021;9:1-
1018 13.

1019 43. Starikova EV, Tikhonova PO, Prianichnikov NA, Rands CM, Zdobnov EM, Ilina EN, et al. Phigaro:
1020 high-throughput prophage sequence annotation. Bioinformatics. 2020;36(12):3882-4.

1021 44. Brown CL, Mullet J, Hindi F, Stoll JE, Gupta S, Choi M, et al. mobileOG-db: a manually curated
1022 database of protein families mediating the life cycle of bacterial mobile genetic elements. Appl Environ
1023 Microbiol. 2022;88(18):e00991-22.

1024 45. R Core Team. R: A language and environment for statistical computing. R Foundation for
1025 Statistical Computing, Vienna, Austria: URL http://www.R-project.org/; 2014.

1026 46. Frerebeau N, Lebrun B, Arel-Bundock V. khroma: Colour Schemes for Scientific Data
1027 Visualization. 2019.

1028 47. Wachi N, Nomano FY, Mitsui H, Kasuya N, Kimura MT. Taxonomy and evolution of putative
1029 thelytokous species of *Leptopilina* (Hymenoptera: Figitidae) from Japan, with description of two new
1030 species. Entomol Sci. 2015;18(1):41-54.

1031 48. Chen F, Schenkel M, Geuverink E, van de Zande L, Beukeboom LW. Absence of complementary
1032 sex determination in two *Leptopilina* species (Figitidae, Hymenoptera) and a reconsideration of its
1033 incompatibility with endosymbiont-induced thelytoky. Insect Sci. 2022;29(3):900-14.

1034 49. Ma WJ, Schwander T. Patterns and mechanisms in instances of endosymbiont-induced
1035 parthenogenesis. J Evol Biol. 2017;30(5):868-88.

1036 50. Jervis MA, Heimpel GE, Ferns PN, Harvey JA, Kidd NA. Life-history strategies in parasitoid
1037 wasps: a comparative analysis of 'ovigeny'. J Anim Ecol. 2001;70(3):442-58.

1038 51. Doremus MR, Stouthamer CM, Kelly SE, Schmitz-Esser S, Hunter MS. Quality over quantity:
1039 unraveling the contributions to cytoplasmic incompatibility caused by two coinfecting *Cardinium*
1040 symbionts. Heredity. 2022;128(3):187-95.

1041 52. Duron O, Bouchon D, Boutin S, Bellamy L, Zhou L, Engelstädter J, et al. The diversity of
1042 reproductive parasites among arthropods: *Wolbachia* do not walk alone. BMC Biol. 2008;6(1):1-12.

1043 53. Kageyama D, Narita S, Watanabe M. Insect sex determination manipulated by their
1044 endosymbionts: incidences, mechanisms and implications. Insects. 2012;3(1):161-99.

1045 54. Perlmutter JI, Bordenstein SR. Microorganisms in the reproductive tissues of arthropods. Nat Rev
1046 Micro. 2020;18(2):97-111.

1047 55. Hopper KR, Wang X, Kenis M, Seehausen ML, Abram PK, Daane KM, et al. Genome divergence
1048 and reproductive incompatibility among populations of *Ganaspis* near *brasiliensis*. G3: Genes, Genomes,
1049 Genetics. 2024:jkae090.

1050 56. Cameron SL. Insect mitochondrial genomics: implications for evolution and phylogeny. Annu Rev
1051 Entomol. 2014;59(1):95-117.

1052 57. Khan S, Sowpati DT, Srinivasan A, Soujanya M, Mishra RK. Long-read genome sequencing and
1053 assembly of *Leptopilina boulardi*: a specialist *Drosophila* parasitoid. G3: Genes, Genomes, Genetics.
1054 2020;10(5):1485-94.

1055 58. Kraaijeveld K, Anvar SY, Frank J, Schmitz A, Bast J, Wilbrandt J, et al. Decay of sexual trait
1056 genes in an asexual parasitoid wasp. Genome Biol Evol. 2016;8(12):3685-95.

1057 59. Wey B, Heavner ME, Wittmeyer KT, Briese T, Hopper KR, Govind S. Immune suppressive
1058 extracellular vesicle proteins of *Leptopilina heterotoma* are encoded in the wasp genome. G3: Genes,
1059 Genomes, Genetics. 2020;10(1):1-12.

1060 60. Fricke LC, Lindsey AR. Identification of parthenogenesis-inducing effector proteins in *Wolbachia*.
1061 Genome Biol Evol. 2024:evae036.

1062 61. Lindsey ARI, Werren JH, Richards S, Stouthamer R. Comparative genomics of a
1063 parthenogenesis-inducing *Wolbachia* symbiont. G3: Genes|Genomes|Genetics. 2016;6(7):2113-23. Epub
1064 2016/05/20. doi: 10.1534/g3.116.028449. PubMed PMID: 27194801; PubMed Central PMCID:
1065 PMCPMC4938664.

1066 62. Kaur R, Shropshire JD, Cross KL, Leigh B, Mansueto AJ, Stewart V, et al. Living in the
1067 endosymbiotic world of *Wolbachia*: A centennial review. Cell Host & Microbe. 2021;29(6):879-93.
1068 PubMed Central PMCID: PMC8192442.

1069 63. Lindsey ARI. Sensing, Signaling, and Secretion: A review and analysis of systems for regulating
1070 host interaction in *Wolbachia*. Genes. 2020;11(7):813. PubMed Central PMCID: PMC7397232.

1071 64. Bordenstein SR, Bordenstein SR. Eukaryotic association module in phage WO genomes from
1072 *Wolbachia*. Nat Commun. 2016;7.

1073 65. Li C, Li C-Q, Chen Z-B, Liu B-Q, Sun X, Wei K-H, et al. *Wolbachia* symbionts control sex in a
1074 parasitoid wasp using a horizontally acquired gene. Curr Biol. 2024.

1075 66. Beckmann JF, Bonneau M, Chen H, Hochstrasser M, Poinsot D, Merçot H, et al. The toxin–
1076 antidote model of cytoplasmic incompatibility: genetics and evolutionary implications. Trends Genet.
1077 2019;35(3):175-85. PubMed Central PMCID: PMC6519454

1078 67. Schilthuizen M, Nordlander G, Stouthamer R, van Alphen J. Morphological and molecular
1079 phylogenetics in the genus *Leptopilina* (Hymenoptera: Cynipoidea: Eucoilidae). Syst Entomol.
1080 1998;23(3):253-64.

1081 68. Vet LE, van Alphen JJ. A comparative functional approach to the host detection behaviour of
1082 parasitic wasps. 1. A qualitative study on Eucoilidae and Alysiinae. Oikos. 1985:478-86.

1083 69. Kanzaki N, Tsai IJ, Tanaka R, Hunt VL, Liu D, Tsuyama K, et al. Biology and genome of a newly
1084 discovered sibling species of *Caenorhabditis elegans*. Nat Commun. 2018;9(1):3216.

1085 70. Koehler G, Khaing KPP, Than NL, Baranski D, Schell T, Greve C, et al. A new genus and species
1086 of mud snake from Myanmar (Reptilia, Squamata, Homalopsidae). Zootaxa. 2021;4915(3):zootaxa.
1087 4915.3. 1-zootaxa. .3. 1.

1088 71. Köhler G, Vargas J, Than NL, Schell T, Janke A, Pauls SU, et al. A taxonomic revision of the
1089 genus Phrynoglossus in Indochina with the description of a new species and comments on the
1090 classification within Occidozyginae (Amphibia, Anura, Dicroglossidae). Vertebrate Zoology. 2021;71:1-26.

1091 72. Köhler G, Zwitzers B, Than NL, Gupta DK, Janke A, Pauls SU, et al. Bioacoustics reveal hidden
1092 diversity in frogs: Two new species of the genus Limnonectes from Myanmar (Amphibia, Anura,
1093 Dicroglossidae). Diversity. 2021;13(9):399.

1094 73. Sullivan JP, Hopkins CD, Pirro S, Peterson R, Chakona A, Mutizwa TI, et al. Mitogenome
1095 recovered from a 19th Century holotype by shotgun sequencing supplies a generic name for an orphaned
1096 clade of African weakly electric fishes (Osteoglossomorpha, Mormyridae). ZooKeys. 2022;1129:163.

1097 74. Brandão-Dias PF, Zhang YM, Pirro S, Vinson CC, Weinersmith KL, Ward AK, et al. Describing
1098 biodiversity in the genomics era: A new species of Nearctic Cynipidae gall wasp and its genome. Syst
1099 Entomol. 2022;47(1):94-112.

1100 75. Heckenhauer J, Razuri-Gonzales E, Mwangi FN, Schneider J, Pauls SU. Holotype sequencing of
1101 *Silvatares holzenthali* Rázuri-Gonzales, Ngera & Pauls, 2022 (Trichoptera, Pisuliidae). ZooKeys.
1102 2023;1159:1.

1103 76. Pohl H, Niehuis O, Gloyna K, Misof B, Beutel RG. A new species of *Mengenilla* (Insecta,
1104 Strepsiptera) from Tunisia. ZooKeys. 2012;(198):79.

1105 77. Rázuri-Gonzales E, Graf W, Heckenhauer J, Schneider JV, Pauls SU. A new species of
1106 *Rhyacophila* Pictet, 1834 (Trichoptera, Rhyacophilidae) from Corsica with the genomic characterization of
1107 the holotype. ZooKeys. 2024;1218:295.

1108 78. Wilder J, Dyreson E, O'Neill R, Spangler M, Gupta R, Wilder A, et al. Contrasting modes of
1109 natural selection acting on pigmentation genes in the *Drosophila dunni* subgroup. Journal of Experimental
1110 Zoology Part B: Molecular and Developmental Evolution. 2004;302(5):469-82.

1111 79. Sugumaran M, Barek H. Critical analysis of the melanogenic pathway in insects and higher
1112 animals. International Journal of Molecular Sciences. 2016;17(10):1753.

1113 80. Dolezal T. How to eliminate pathogen without killing oneself? Immunometabolism of
1114 encapsulation and melanization in *Drosophila*. Frontiers in Immunology. 2023;14:1330312.

1115 81. Carton Y, Poirié M, Nappi AJ. Insect immune resistance to parasitoids. Insect Sci. 2008;15(1):67-
1116 87.

1117 82. Russo J, Dupas S, Frey F, Carton Y, Brehelin M. Insect immunity: early events in the
1118 encapsulation process of parasitoid (*Leptopilina boulardi*) eggs in resistant and susceptible strains of
1119 *Drosophila*. Parasitology. 1996;112(1):135-42.

1120 83. Dombeck I, Jaenike J. Ecological genetics of abdominal pigmentation in *Drosophila falleni*: a
1121 pleiotropic link to nematode parasitism. Evolution. 2004;58(3):587-96.

1122 84. Siva–Jothy MT. A mechanistic link between parasite resistance and expression of a sexually
1123 selected trait in a damselfly. Proceedings of the Royal Society of London Series B: Biological Sciences.
1124 2000;267(1461):2523-7.

1125 85. Wilson K, Cotter SC, Reeson AF, Pell JK. Melanism and disease resistance in insects. Ecol Lett.
1126 2001;4(6):637-49.

1127 86. Tan S, Wang Y, Liu P, Ge Y, Li A, Xing Y, et al. Increase of albinistic hosts caused by gut
1128 parasites promotes self-transmission. Frontiers in Microbiology. 2018;9:1525.

1129 87. Lindsey E, Altizer S. Sex differences in immune defenses and response to parasitism in monarch
1130 butterflies. Evol Ecol. 2009;23:607-20.

1131 88. Krams I, Burghardt GM, Krams R, Trakimas G, Kaasik A, Luoto S, et al. A dark cuticle allows
1132 higher investment in immunity, longevity and fecundity in a beetle upon a simulated parasite attack.
1133 Oecologia. 2016;182:99-109.

1134 89. Dubovskiy I, Whitten M, Kryukov V, Yaroslavtseva O, Grizanova E, Greig C, et al. More than a
1135 colour change: insect melanism, disease resistance and fecundity. Proc R Soc Lond B.
1136 2013;280(1763):20130584.

1137 90. Wittkopp PJ, Beldade P, editors. Development and evolution of insect pigmentation: genetic
1138 mechanisms and the potential consequences of pleiotropy. Semin Cell Dev Biol; 2009: Elsevier.

1139 91. Kohler LJ, Carton Y, Mastore M, Nappi AJ. Parasite suppression of the oxidations of eumelanin
1140 precursors in *Drosophila melanogaster*. Archives of Insect Biochemistry and Physiology: Published in
1141 Collaboration with the Entomological Society of America. 2007;66(2):64-75.

1142 92. Stouthamer R, Russell JE, Vavre F, Nunney L. Intragenomic conflict in populations infected by
1143 Parthenogenesis Inducing *Wolbachia* ends with irreversible loss of sexual reproduction. BMC Evol Biol.
1144 2010;10:12. doi: 10.1186/1471-2148-10-229. PubMed PMID: WOS:000282746700002.

1145 93. Ma W-J, Pannebakker BA, Li X, Geuverink E, Anvar SY, Veltsos P, et al. A single QTL with large
1146 effect is associated with female functional virginity in an asexual parasitoid wasp. Mol Ecol.
1147 2021;30(9):1979-92. doi: https://doi.org/10.1111/mec.15863.

1148 94. Ma WJ, Pannebakker BA, Beukeboom LW, Schwander T, van de Zande L. Genetics of decayed
1149 sexual traits in a parasitoid wasp with endosymbiont-induced asexuality. Heredity. 2014;113(5):424-31.
1150 doi: 10.1038/hdy.2014.43. PubMed PMID: 24781809; PubMed Central PMCID: PMC4220718.

1151 95. Russell JE, Stouthamer R. The genetics and evolution of obligate reproductive parasitism in
1152 *Trichogramma pretiosum* infected with parthenogenesis-inducing *Wolbachia*. Heredity. 2011;106(1):58-
1153 67. doi: 10.1038/hdy.2010.48. PubMed PMID: WOS:000285336100007.

1154 96. Gottlieb Y, Zchori-Fein E. Irreversible thelytokous reproduction in *Muscidifurax uniraptor*. Entomol
1155 Exp Appl. 2001;100(3):271-8.

1156 97. Stouthamer R, Mak F. Influence of antibiotics on the offspring production of the *Wolbachia*-
1157 infected parthenogenetic parasitoid *Encarsia formosa*. J Invertebr Pathol. 2002;80(1):41-5.

1158 98. van der Kooi CJ, Schwander T. On the fate of sexual traits under asexuality. Biol Rev Camb
1159 Philos Soc. 2014;89(4):805-19. doi: 10.1111/brv.12078. PubMed PMID: 24443922.

1160 99. Neiman M, Sharbel TF, Schwander T. Genetic causes of transitions from sexual reproduction to
1161 asexuality in plants and animals. J Evol Biol. 2014;27(7):1346-59. doi: 10.1111/jeb.12357. PubMed PMID:
1162 24666600.

1163 100. van der Kooi CJ, Matthey-Doret C, Schwander T. Evolution and comparative ecology of
1164 parthenogenesis in haplodiploid arthropods. Evolution Letters. 2017;1(6):304-16.

1165 101. Vrijenhoek RC, Parker ED. Geographical parthenogenesis: general purpose genotypes and
1166 frozen niche variation. Lost sex: the evolutionary biology of parthenogenesis. 2009:99-131.

1167 102. Hörandl E. Geographical parthenogenesis: opportunities for asexuality. Lost sex: The
1168 evolutionary biology of parthenogenesis. 2009:161-86.

1169 103. Gillespie RG. Island time and the interplay between ecology and evolution in species
1170 diversification. Evolutionary Applications. 2016;9(1):53-73.

1171 104. Lindsey ARI, Rice DW, Bordenstein SR, Brooks AW, Bordenstein SR, Newton ILG. Evolutionary
1172 genetics of cytoplasmic incompatibility genes *cifA* and *cifB* in prophage WO of *Wolbachia*. Genome Biol
1173 Evol. 2018;10(2):434-51. doi: 10.1093/gbe/evy012. PubMed Central PMCID: PMCPMC5793819.

1174 105. Verhulst EC, Pannebakker BA, Geuverink E. Variation in sex determination mechanisms may
1175 constrain parthenogenesis-induction by endosymbionts in haplodiploid systems. Current Opinion in Insect
1176 Science. 2023:101023.
1177